Research Square

Preprints are preliminary reports that have not undergone peer review.
They should not be considered conclusive, used to inform clinical practice,
or referenced by the media as validated information.

Chitosan Nanoparticles as Smart Carriers of Hexaconazole for managing rice blast incited by Pyricularia oryzae Cavara

N. Kiran Kumar
n.kirankumar@angrau.ac.in

ANGRAU
P. Anil Kumar
ANGRAU Advanced Post Graduate Centre
P. Madhusudhan
ANGRAU Agricultural Research Station
Ch. Sreenivasa Rao
ANGRAU
B. Sreekanth
ANGRAU Regional Agricultural Research Station
T. N.V.K.V. Prasad
ANGRAU Regional Agricultural Research Station
G. S. Jasudasu
ICAR-Indian Institute of Rice Research
Devaki K
ANGRAU Regional Agricultural Research Station

Research Article

Keywords: Chitosan encapsualtion, Disease management, Hexaconazole, Rice, EC50, Mass Spectrometry

Posted Date: March 4th, 2026

DOI: https://doi.org/10.21203/rs.3.rs-8838112/v1

License: This work is licensed under a Creative Commons Attribution 4.0 International License. Read Full License

Additional Declarations: No competing interests reported.

Abstract

Rice blast, caused by the fungal pathogen *Pyricularia oryzae*, remains a major constraint on global rice production, significantly affecting yield and quality. In our previous study in evaluating the efficacy of various fungicides on *P. oryzae*; hexaconazole emerged as the most potent antifungal agent. Hence, in the current study, hexaconazole was further encapsulated in the nano particles of a bio-macromolecule, chitosan (HECNPs) and characterized using scanning electron microscopy (SEM), energy-dispersive X-ray spectroscopy (EDS), Fourier-transform infrared spectroscopy (FTIR), dynamic light scattering (DLS), zeta potential and gas chromatography-mass spectrometry (GC-MS) analysis. These assessments confirmed the successful synthesis of nano-formulated hexaconazole, exhibiting superior stability and controlled release properties when compared to commercial hexaconazole. The half maximal effective concentration (EC_{50}) of hexaconazole and HECNPs were found to be 800 ppm and 200 ppm, respectively. The dissipation of hexaconazole in paddy leaves sprayed with HECNPs were quantified at 0, 5, 10 and 15 days and observed the improved dissipation dynamics of HECNPs over commercial hexaconazole. Field experiments and Uniform Blast Nursery (UBN) trials validated the superior performance of HECNPs in disease suppression and yield improvement. The application of HECNPs at a rate of 12.5 g active ingredient (a.i.) per hectare with two foliar sprays achieved the lowest disease incidence of 25.1% and highest yield of 3166.6 kg ha^{-1} leading to the highest net returns per rupee invested (NRRI) of 3.66 in season 1 and 3.53 in season 2. These findings confirm that nano-encapsulation technology using HECNP enhances disease management besides aiding economic feasibility of rice blast management strategies.

Introduction

Rice (*Oryza sativa* L.), a staple food for over half of the world's population, plays a crucial role in global food security and the agricultural economy with a productivity average of 4.4 tons per hectare [84]. Rice cultivation underpins the livelihoods of millions, however, this essential crop faces significant threats from various biotic factors, especially rice blast disease, which is caused by the hemi-biotrophic, filamentous recalcitrant fungus *Pyricularia oryzae* Cavara (teleomorph: *Magnaporthe oryzae* B.C.Couch). This disease is particularly insidious, capable of infecting rice plants at all growth stages thus resulting in devastating yield losses up.to 100% under favourable conditions for the pathogen [57, 64]. Given that rice is central to food security in many regions, managing its vulnerabilities is of paramount importance.

Rice blast disease can severely compromise the structural integrity of the rice plant by affecting various parts, including leaves, stems, nodes and panicles. Infection in the vegetative phase is referred to as ‘leaf blast’, while infection in the nodes and neck of panicles during the reproductive phase is referred to as ‘node’ and ‘neck blast’, respectively [11]. All growth stages of rice are vulnerable to leaf blast disease, although the seedling, early tillering and heading stages are most vulnerable [7].

The pathogen's adaptability and genetic diversity pose significant challenges to conventional management strategies. These strategies often rely heavily on the use of chemical fungicides and the cultivation of resistant crop varieties. While these methods can be effective to a certain level, their limitations are becoming increasingly apparent. The reliance on fungicides raises environmental concerns, including potential toxicity to non-target organisms and contamination of soil and water resources. Additionally, the constant application of fungicides can select for resistant strains of the pathogen, diminishing the fungicidal efficacy over time [40, 53].

In light of these challenges, the search for novel fungicidal treatments remains an essential avenue for ensuring sustainable rice production. The melanin biosynthesis inhibitor fungicide, tricyclazole, has been often used for the management of blast disease for four decades [23, 27]. In addition to tricyclazole, metominostrobin, pyraclostrobin, azoxystrobin, carbendazim, pyroquilon, isoprothiolane, propiconazole and tebuconazole were being used for controlling rice blast [5, 71, 90]. Current options like tricyclazole, carbendazim and mancozeb have shown promise but became worrisome by issues of resistance and regulatory bans in some regions due to their long-term residual effects [40, 52, 53]. Therefore, the exploration of alternative fungicides that can effectively manage rice blast disease without fostering resistance by evaluating their *in- vitro*

efficacy against *P. oryzae* is of critical importance [22]. This current study aims to evaluate such fungicides, contributing valuable insights into the development of more effective and sustainable management strategies for rice blast disease.

Nanoparticles (NPs) possess high reactivity, require only small quantities, and allow precise delivery and controlled release of active ingredients in plants, making them highly effective as pesticides and fertilizers [20, 61]. Carbon, silver, silica, and non-metal oxides such as alumino-silicate NPs are particularly reactive and can efficiently penetrate microbial cells even at low concentrations, thereby exerting strong antimicrobial effects [4, 54, 76].

Research evidence indicates that nanosized materials often exhibit unique properties, with chitosan-based nanoparticles (NPs) gaining significant attention due to their biodegradability, stability, and eco-friendliness. Derived from chitin, chitosan is a cationic, biocompatible polysaccharide with pH-sensitive properties. Since their first characterization, chitosan NPs have found applications in medicine, agriculture, and environmental management [63]. Their synthesis methods, such as ionic gelation and electrospraying, directly influence their functionality. In agriculture, chitosan NPs provide antimicrobial and antifungal benefits, thereby strengthening crop protection. Other polymeric nanocarriers, including polylactic-co-glycolic acid [9] and zirconium NPs [83] have also demonstrated potential in the controlled delivery of fungicides such as propiconazole and tebuconazole, respectively thus ensuring high efficacy with reduced toxicity and minimal environmental impact.

Microorganisms that exhibit reduced sensitivity to antibiotics due to poor cellular penetration can be managed more effectively using nano-formulations [76]. Addressing the challenge of rice blast disease, recent nanotechnology advancements, particularly nanoformulations based on bio-macromolecules like chitosan offer novel and promising solutions. Nano-fungicides, which incorporate nanoscale carriers, enhance both the stability and efficacy of conventional fungicides such as thiophanate-methyl, benomyl, carbendazim, prochloraz, and propiconazole, which target fungal β-tubulin and ergosterol biosynthesis pathways. Nano-encapsulation techniques, involving carriers like graphene oxide, mesoporous organo-silica, and polylactic acid NPs, enable targeted delivery and controlled release of fungicides, facilitating deeper penetration into fungal pathogens such as *Rhizoctonia solani*, *Sclerotinia sclerotiorum*, and *Fusarium* spp. [25, 59, 77]. This approach allows for lower application rates while maintaining or even enhancing fungicidal efficacy, thereby reducing environmental risks and minimizing the chances of resistance development in fungal populations [3, 58, 75]. In this context, the present research represents the first attempt to encapsulate hexaconazole within chitosan nanoparticles. The aim is to develop a comprehensive disease management strategy by enabling the controlled release of hexaconazole from chitosan NPs, thereby significantly reducing the impact of rice blast under field conditions.

Material and methods

The present study was performed at the Department of Plant Pathology, Agricultural College, Bapatla, while field trials were carried out at the Agricultural Research Station, Nellore (hotspot for leaf blast) during *rabi*, 2022-23 and *rabi*, 2023-24. The virulent isolate of *P. oryzae* on which hexaconazole was found to be effective in our previous study [42] was used in the current study.

PREPARATION OF HEXACONAZOLE ENCAPSULATED CHITOSAN NANOPARTICLES (HECNPS) AND CHITOSAN NANO PARTICLES (CNPS)

Chemicals and Reagents

Hexaconazole ($C_{14}H_{17}Cl_2N_3O$, with the molecular weight of 314.21 g/mol and the purity of 99.7%) was procured from Dr.Ehrenstorfer, Germany and was used as received. Chitosan (low molecular weight), acetic acid glacial (100%) and Tween-80 were purchased from Sigma Aldrich (St. Louis, MO, USA). Hydrochloric acid (37%), HPLC grade water and *N,N*-

dimethylformamide (DMF) were purchased from Himedia, Mumbai and Merck, USA, respectively. The organic solvents, specifically HPLC grade ethyl acetate alongside various chemical agents, including primary secondary amine (PSA), graphitized carbon black (GCB) nano powder, sodium chloride (NaCl), anhydrous magnesium sulfate ($MgSO_4$) and anhydrous sodium sulfate (Na_2SO_4) procured from Merck (Mumbai, India) were used in the current study. The $MgSO_4$ was baked for 5 h at 500ºC in the muffle furnace to remove phthalates and residual water. All other reagents used were of analytical grade.

Hexaconazole encapsulated chitosan nanoparticles (HECNPs) were prepared using ionic gelation method with slight modifications (Fig. 1) [17]. Chitosan, 0.5 g was dissolved in 100 mL of 1.0% (*v/v*) acetic acid solution and stirred continuously at 120 rpm for 2 h. Due to its low water solubility, 1 g of hexaconazole was dissolved in 100 mL of N,N-Dimethylformamide (DMF). The HECNPs were prepared by adding hexaconazole-DMF drop wise to the chitosan solution which is at continuous stirring at 120 rpm and left undisturbed for overnight under stirring on magnetic stirrer. The pH of the resulting mixture was around 3.6 and is adjusted to 6.5 by using 0.1 M NaOH. Then, 2% *v/v* of TWEEN-80 was added as a stabilizer. The concentration of hexaconazole was determined by using GC-MS analysis as detailed in the below paragraphs. The desired concentrations of 200 ppm were prepared by diluting the obtained HECNPs with HPLC grade water and subsequently determining the concentration of hexaconazole by using GC-MS. The prepared HECNPs were stored at 4^oC for further analysis. The chitosan nano particles (CNPs) were prepared by following the above procedure without adding hexaconazole.

In-vitro Antifungal Assay

To determine the effective concentration of commercial hexaconazole 5% EC (Contaf) and HECNPs, an *in vitro* antifungal assay against *P. oryzae* was conducted using the poisoned food technique. A stock solution of 10,000 ppm was prepared for both hexaconazole and HECNPs. The initial concentrations of HECNPs were determined by GC-MS analysis and subsequently diluted to the desired concentrations using HPLC-grade water. The final concentrations were reconfirmed via GC-MS analysis. The experiment followed a completely randomized design (CRD) under laboratory conditions. Potato dextrose agar (PDA) was amended with commercial hexaconazole and HECNPs at varying concentrations (125, 250, 500, 1000, 1500, and 2000 ppm). PDA without fungicide served as the control. The prepared medium was poured into sterile Petri plates and allowed to solidify. A seven mm mycelial disc, taken from the margin of a seven-day old *P. oryzae* culture, was aseptically placed at the center of each amended PDA plate. The plates were incubated at 25 ± 2°C and radial mycelial growth was measured every two days for 15 days. Each treatment was replicated five times. The percentage inhibition (I) of radial growth was calculated using formula given by Vincent (1947): Inhibition (%) = [(radial growth in control – radial growth in treatment)/ radial growth in control] x 100.

Determination of EC values

The EC_{50} values, representing the effective fungicide concentration (in µg/mL) required to inhibit 50% of mycelial growth, were determined by converting fungicide concentrations into logarithmic values and analyzing fungal relative growth data. The EC_{50} values for hexaconazole and synthesized HECNPs were calculated using R software, with log-transformed concentrations plotted on the X-axis and their corresponding probit values on the Y-axis.

CHARACTERIZATION OF HECNPs

Scanning Electron Microscopic (SEM) with Energy Dispersive Spectroscopy (EDS) Analysis

The surface topology and size of HECNPs were analyzed using a scanning electron microscope (SEM) with a CARL-ZEISS AG-ULTRA 55 machine equipped with an energy dispersive spectroscopy (EDS) analyzer. This analysis was performed to

determine the size, shape, and elemental distribution of HECNPs. A 2 µL sample of the encapsulation complex was placed on a stub, air-dried for 1 minute, and then subjected to gold sputtering using a sputter coater (EMITECH K-550X; Ashford, UK). The prepared specimen was then analyzed under SEM, and images were captured at various magnifications.

Hydrodynamic Diameter and Zeta Potential Analysis

The mean hydrodynamic diameter, zeta potential, and polydispersity index of HECNPs in carboxymethyl cellulose (CMC; 0.1% w/v) were assessed using dynamic light scattering (DLS) with a zeta sizer (Nanopartica®, HORIBA, SZ-100; Kyoto, Japan). The instrument was equipped with a 10 mW or 100 mW laser beam at a wavelength of 532 nm. The surface charge of HECNPs was measured using an electrophoretic light scattering technique with a fold capillary cuvette. Zeta potential measurements were conducted at 25°C with an electrode voltage of 3.9 V.

Fourier Transform Infrared (FT-IR) Spectroscopy Analysis

FT-IR spectroscopy was used to identify the functional groups present in the synthesized nanoparticles. FT-IR spectral analysis of CNPs and HECNPs was conducted using an FT-IR 6600 spectrometer (Jasco Corporation, Tokyo, Japan) over a wavelength absorption range of 4500 to 350 cm^{-1}. Potassium bromide (KBr) was used to prepare compressed sample discs. The analysis was performed with 16 scans at a resolution of 4 cm^{-1} and a scanning speed of 2 mm per second.

Gas Chromatography and Mass Spectrometry- Mass Spectrometry (GC-MS/MS) analysis

Apparatus

Gas chromatograph (Nexis GC-2030), coupled with the gas chromatograph mass spectrometer (GCMS) featuring a triple quadrupole detector (TQ8040 NX) equipped with an autosampler (AOC-20 s plus) and an auto injector (AOC-20i plus) for further enhancing the automation and minimizing the human error thereby increasing throughput efficiency were used in the current study. A SH-Rxi-5Sil MS capillary column, characterized by its dimensions of 30 m × 0.25 mm I.D. and a film thickness of 0.25 µm, is used to facilitate the separation of analytes at elevated temperatures, ranging from 320 to 350ºC. The above apparatus is procured from Shimadzu, Japan.

Method Validation

The method was validated for determination of hexaconazole residues in paddy leaf samples. The parameters includes linearity, Limit of Detection (LOD), Limit of Quantification (LOQ), recovery, repeatability, matrix effect (ME), ion ratio and retention time. The linearity of the method was evaluated by analysing the hexaconazole at five concentrations in the range of 0.01–1.0 µg/mL. The LOD and LOQ of the method was determined by considering the signal to noise (S/N) ratio of > 3:1 and 10:1, respectively with regarding the background noise obtained from the paddy leaf samples. Individual stock standard solutions (1 mg/mL) were prepared in ethyl acetate and stored in the dark at − 20°C. Prior to their use, they were kept for 1 h at ambient temperature. A standard stock solution of pesticides was prepared in ethyl acetate at 10 µg /mL with respect to hexaconazole. Spiked calibration curves at 5 levels of 10, 20, 30, 50, and 100 ng/g in triplicates were prepared by addition of 10 µL, 20 µL, 30 µL, 50 µL and 100 µL of mixed standard stock solution, respectively, to 10 g portions of blank paddy leaf samples in each case. The control sample was also maintained simultaneously to compare the interference with standard spiked samples. The spiked samples were processed using the validated methodology. The repeatability of the analytical method was evaluated in terms of relative standard deviation (RSD). The matrix effect was carried out to determine the suppression and enhancement of signal matrix effects. This was done to avoid false positive analytical reports. The matrix effect (ME) was determined by using formula: ME(%)= [(Peak area of matrix standard – Peak area of solvent standard)/ Peak area of matrix standard]×100. The retention of analytes was verified from the solvent and matrix match standards

solutions. The ion ratio value was calculated from GC–MS data by using the formula [Ion ratio: (Peak area confirmation ion) × 100/peak area (quantitation ion)].

Sample preparation

Sample preparation was carried out by using AOAC- Quick, Easy, Cheap, Effective, Rugged, and Safe (QuEChERS) method with slight modifications [69]. The paddy leaf samples of 1000 g were finely homogenized in the blixer (Robot coupe make, France). After obtaining homogeneate from each sample the blixer bowl, blades and lid with arm were cleaned thoroughly with water, shade dried and used for other samples inorder to remove the remnants of previous samples.

Extraction

The finely pulverized leaf sample (10 g) was taken to 50 mL falcon tubes and added with 10 mL HPLC grade water and 20 mL ethyl acetate. The samples were then thoroughly homogenized in the homogenizer (Unidrive X 1000D (CAT Make, Ballrechten-Dottingen, Germany)). To the homogenate NaCl (3 g) was added and the mixture was mixed at high speed with vortex mixer for 1min. The mixture was centrifuged at 3000 rpm for 3 min.

d-SPE cleanup (removal of fatty acids, sugars, ionic-lipids and non-polar pigments)

Supernatant (12 mL) was collected and transferred to the falcon tubes containing activated anhydrous Na_2SO_4 (5 g) was added to the mixture, and mixing was continued in vortex for an additional 1 min. The supernatant (9 mL) was transferred to a 15 mL falcon tube containing PSA (0.2 g), $MgSO_4$ (0.6 g) and GCB (200 mg). After shaking for 1 min and centrifugation for 3 min at 3000 rpm, 1 mL of supernatant was transferred to a 2 mL glass vial through 0.45 µm syringe filter (Merck, PTFE) and thereafter placed in the autosampler and 1 µL of the solution was injected into gas chromatograph at 250°C.

Recovery studies

For recovery determination, spiked blank paddy samples at concentration levels of 30, 60, 150, 250, 350 ng/ g were prepared in triplicates and they were kept for 1 h at ambient temperature prior to their use and then treated according to the procedure described in earlier paragraphs. The recoveries were calculated using the calibration curves constructed using spiked samples. After acquisition of the total ion chromatogram for the mixed stock standard solutions in scan mode, peaks were identified by their retention time and mass spectra. The most abundant ion that showed no evidence of chromatographic interference and had the highest signal-to-noise ratio was selected for quantification purposes.

Determination of hexaconazole concentration in paddy leaf samples

Rice leaf samples were collected from the rice plots (60 days old) sprayed with HECNPs at 200.6 ppm (T1) and hexaconazole (commercial formulation, Contaf) at 802.6 ppm (T2) at ARS, Nellore in Rabi 2023-24 were used in the current study. The leaf samples of 1000 g were collected separately from each treatment at 0 days (immediately after spraying), 5 days, 10 days and 15 days after spraying and the leaf samples collected from unsprayed plot were considered as control. Samples were stored at -4 ºC for further usage.

Gas chromatography-mass spectrometry (GC-MS/MS) analysis

The column oven temperature of GC was programmed as follows: 60°C for 1 min, 60 to 170°C (ramp 40°C/min) for 0 min, 170 to 310°C (ramp 10°C/min) for 3 min. Ultrapure grade Helium (99.9999%) (Bhuruka Gases, Bengaluru, India) was used as carrier gas at constant flow rate of 1.0 mL/min. In the MS, ion source temperature and ionization energy were set at 230°C and 70 eV, respectively. The interface temperature was maintained at 250°C. Target and qualifier ions were selected for each analyte by injecting them mixed under same chromatographic conditions in full-scan mode with a m/z of 25–500. The target analytes were confirmed by similarity match with NIST library. The ions were selected based on relative intensity percentage in the mass spectrum of hexaconazole. Three ions were selected and one for quantification and another two for qualifier

ions. In order to avoid contamination of the samples, injector was washed with ethyl acetate before and after quantitation of hexaconazole residues in each sample.

TESTING THE EFFICACY OF HECNPS IN MANAGING RICE BLAST UNDER FIELD CONDITIONS

The field efficacy of hexaconazole encapsulated in chitosan nanoparticles (HECNPs) in reducing the incidence of rice blast was evaluated over two consecutive cropping seasons: *rabi*, 2022-23 (season 1) and rabi 2023-24 (season 2). The study aimed to determine the effectiveness of HECNPs in controlling the disease and improving rice yield. To ensure the accuracy and reliability of the findings obtained in season 1, the treatments were applied in both the Uniform Blast Nursery (UBN) and the field during season 2. The experiment followed a Randomized Block Design (RBD) with nine treatments *i.e.* T1: HECNPs at 2.5 g a.i. ha^{-1} with 1 spray, T2: HECNPs at 2.5 g a.i. ha^{-1} with 2 sprays, T3: HECNPs at 5.0 g a.i. ha^{-1} with 1 spray, T4: HECNPs at 5.0 g a.i. ha^{-1} with 2 sprays, T5: HECNPs at 12.5 g a.i. ha^{-1} with 1 spray, T6: HECNPs at 12.5 g a.i. ha^{-1} with 2 sprays, T7 : Commercial Hexaconazole at 20.0 g a.i. ha^{-1} (Control), T8 : Carrier Control (Chitosan at 2.0 g L^{-1}) and T9: Control (water) allowing for statistical comparison of different treatments with three replications of each treatment. As a reference for assessing efficacy, the standard recommended dose of commercial hexaconazole @ 20.0 g a.i. ha^{-1} (T8) was used as a control thus providing a standard comparison for the performance of HECNP treatments. Additionally, chitosan nanoparticles (T9) without hexaconazole were incorporated into the study to determine the standalone effectiveness of chitosan nanoparticles in disease management.

The impact of the treatments was evaluated by recording disease incidence and yield attributes for each treatment (Fig. 2). The incidence of rice blast was quantified using the Percent Disease Index (PDI), while grain yield was measured to assess the productivity of the treated plants. Twenty-five-day old rice seedlings were carefully transplanted into the main field, ensuring a uniform spacing of 15 cm × 15 cm within a 4 m × 3 m gross plot size. Proper nutrient management was followed to support plant growth, with the application of 150 kg nitrogen (N), 60 kg phosphorus (P_2O_5), and 50 kg potassium (K_2O) as fertilizers. Prior to transplanting, half of the nitrogen and the full dose of phosphorus and potassium were applied as a basal dose to ensure adequate nutrient availability. The remaining nitrogen was top dressed in two equal splits, administered at the tillering and panicle initiation stages to support crop development and yield potential.

The Uniform Blast Nursery (UBN) was set up to further analyze the treatments under controlled conditions. UBN beds were divided into mini plots, each measuring 1 m × 1 m, ensuring a systematic assessment of disease progression (supplemantary figure). The treatments were applied in the form of foliar sprays, with the first application administered at the initial appearance of the disease and the second spray was applied 15 days after the first spray.

Recording Disease Incidence

In each treatment, fifteen plants were randomly selected per replication for observation, ensuring an unbiased assessment of disease severity. To maintain accuracy, border rows were excluded from the observations, preventing any potential edge effects. The severity of leaf blast was evaluated on two occasions: the day before spraying and 15 days after each spray application, following the Standard Evaluation System (SES) scale developed by IRRI [35] (Supplemantary table). The extent of disease incidence was further quantified using the Percent Disease Index (PDI), which was calculated based on the formula provided by Wheeler (1969) i.e. PDI = (Sum of Individual disease ratings / Number of plants observed x maximum disease rating) x 100.

Area Under Disease Progress Curve (AUDPC)

The effectiveness of various treatments was evaluated by calculating Area Under the Disease Progress Curve (AUDPC) values, following the formula established by Wilcoxson *et al.* [89]. $\mathrm{AUDPC} = \sum_{i=1}^{k} \frac{1}{2}(S_i + S_{i-1}) \times d$

Where, S_i = Disease incidence at i^{th} day of evaluation, k = Number of successive evaluation of the disease, d = Interval between i and i-1evaluation of disease.

Recording Yield and Yield Attributes

The harvesting process was conducted replication-wise, ensuring that only the designated experimental plots were harvested while excluding the border rows to prevent edge effects and maintain data accuracy. After harvesting, the grain yield from the net plot area of each replication was carefully weighed separately for each treatment. The recorded values were then documented as the yield per plot for each respective replication. To determine the overall yield for each treatment, the average grain weight from all three replications of the corresponding treatment was calculated.

STATISTICAL ANALYSIS

Statistical analysis of data from both laboratory and field experiments followed the standard procedures outlined by Gomez and Gomez [28]. Radial growth values were transformed using Box-Cox transformation in R software before being subjected to one-way ANOVA, with mean comparisons conducted using Duncan's Multiple Range Test (DMRT). The half-maximal effective concentration (EC_{50}) of chitosan–hexaconazole nanoparticles was determined using Probit regression in R Studio. The pooled analysis of disease incidence and yield data was performed by applying Atkins transformation, followed by Factorial RBD analysis.

Results and Discussion

In our previous study, hexaconazole was identified as the most effective fungicide against *P. oryzae* under *in-vitro* and in the current study hexaconazole, was encapsulated in chitosan nanoparticles. The synthesis, characterization, and confirmation of these nanoparticles were carried out. Furthermore, the field efficacy of the formulated nanoparticles was assessed both in main field conditions and in a uniform blast nursery. The findings obtained through this research are presented and discussed hereunder.

PREPARATION AND CHARACTERIZATION OF NANO FORMULATIONS AGAINST P. oryzae

In-vitro Efficacy of Hexaconazole on P. oryzae

Various concentrations (2000 ppm, 1500 ppm, 1000 ppm, 500 ppm, 250 ppm, 125 ppm) of both commercial hexaconazole (Contaf) and hexaconazole encapsulated in chitosan nano particles (HECNPs) were evaluated *in vitro* for their efficacy on the growth of *P. oryzae*. Testing of commercial formulations revealed the pronounced concentration-dependent relationship with statistical significance among all the concentrations tested. At the higher concentrations *i.e.* 2000 ppm, 1500 ppm, and 1000 ppm, complete inhibition of *P. oryzae* growth was achieved, indicating potent antifungal activity at these levels. At a concentration of 500 ppm, growth inhibition was reduced to 44.2%, with a corresponding mycelial growth measurement of 50.2 mm. A marked decline in efficacy was observed at lower concentrations of 250 ppm and 125 ppm, with inhibitions recorded at merely 7.8% and 1.9%, respectively (Table 1). These figures suggest that below 500 ppm, the commercial formulation struggles to maintain effective antifungal properties, aligning closely with control growth rates, thereby reflecting the need for higher dosages to achieve significant inhibition.

Table 1
Efficacy of hexaconazole and HECNPs on the growth of *P. oryzae in-vitro*

Tr.No.	Treatments	Commercial formulation		HECNPs	
		Radial growth (in mm)	inhibition over control (%)	Radial growth (in mm)	inhibition over control (%)
T1	Hexaconazole 2000 ppm	0^{a} (0.73)	100.0	0.0^{a} (0.66)	100.0
T2	Hexaconazole 1500 ppm	0^{a} (0.73)	100.0	0.0^{a} (0.66)	100.0
T3	Hexaconazole 1000 ppm	0^{a} (0.73)	100.0	0.0^{a} (0.66)	100.0
T4	Hexaconazole 500 ppm	50.2^{b} (5.76)	44.2	9.0^{b} (1.53)	89.8
T5	Hexaconazole 250 ppm	83.0^{c} (6.83)	7.8	23.8^{c} (2.56)	73.4
T6	Hexaconazole 125 ppm	88.2^{c} (6.97)	1.9	61.8^{cd} (3.13)	30.8
T7	Control	90^{c} (7.01)	-	89.3^{d} (3.33)	-
SE(m) (±)		0.088	-	0.2	-
CD (P ≤ 0.01)		0.259	-	0.592	-
CV (%)		4.25	-	2.232	-
Figures in the parenthesis are Box-Cox transformed values. λ = 0.1818182 (for commercial formulation),					
λ< -0.1414141 (chitosan NPs encapsulated formulation					

The HECNPs formulation exhibited a remarkable performance comparable to the commercial formulations at the highest concentrations. Like the commercial product, cent per cent inhibition was observed at 2000 ppm, 1500 ppm, and 1000 ppm. However, at the mid-range concentration of 500 ppm, HECNPs demonstrated a substantial 89.8% growth inhibition, with a mycelial growth measurement markedly reduced to 9.0 mm (Table 1). This exceptional performance indicated that chitosan NPs could enhance the bioavailability and efficacy of hexaconazole, potentially leading to reduced dosage requirements for effective blast management. Further analysis showed that at 250 ppm, growth inhibition was 73.4%, showcasing a significant antifungal effect, while at 125 ppm, 30.8% inhibition was observed, correlating with mycelial growth of 23.8 mm and 61.8 mm, respectively. Interestingly, a significant difference was evident between the growth responses at these concentrations and the control, underscoring the potential of HECNPs formulation to maintain efficacy at lower concentration thresholds compared to the commercial formulations.

This study evaluated the antifungal efficacy of various concentrations of commercial hexaconazole and HECNPs formulation of hexaconazole against *P. oryzae in vitro*. The results highlight a clear concentration-dependent relationship for

both formulations, with significant differences observed at all tested concentrations. The findings are supported by published research, which emphasizes the potential of nanoparticle based delivery systems to enhance the bioavailability and efficacy of fungicides [41, 46].

The commercial formulation exhibited a concentration-dependent inhibition of *P. oryzae*, a trend that has been widely reported in studies on chemical fungicides [62]. At the highest concentrations tested (2000 ppm, 1500 ppm, and 1000 ppm), complete inhibition of fungal growth was observed, emphasizing the formulation's potent antifungal activity. These findings align with the work of Nirmal and Shambhu [60], who demonstrated similar efficacy of triazole fungicides against rice blast pathogen at high dosages.

At 500 ppm, the inhibition decreased significantly to 44.2%, with a mycelial growth measurement of 50.2 mm. This reduction in efficacy at lower concentrations corroborates findings by Matei *et al.* [49], who reported that the performance of conventional fungicides diminishes below a critical threshold, limiting their utility in low-dose applications. In our study, at even lower concentrations (250 ppm and 125 ppm), the inhibition rates dropped sharply to 7.8% and 1.9%, respectively, indicating that the commercial formulation struggles to maintain effective antifungal properties under these conditions. This limitation emphasizes the need for higher dosages to achieve substantial inhibition, as highlighted by Gupta *et al.* [30].

The HECNPs formulation exhibited superior performance across all tested concentrations, demonstrating exceptional efficacy against *P. oryzae*. At higher concentrations of 2000 ppm, 1500 ppm, and 1000 ppm, the formulation achieved complete inhibition, matching the performance of the commercial product. At 500 ppm, however, HECNPs significantly outperformed the commercial counterpart, achieving an inhibition rate of 89.8% with a mycelial growth measurement of just 9.0 mm. This enhanced performance is attributed to the improved delivery and bioavailability of hexaconazole facilitated by its encapsulation in chitosan nanoparticles [46, 51].

Even at lower concentrations, the HECNPs formulation consistently outperformed the commercial product. At 250 ppm, it achieved a notable 73.4% inhibition with a mycelial growth of 23.8 mm, significantly surpassing the commercial product's inhibition rate of 7.8% at the same concentration. Similarly, at 125 ppm, HECNPs achieved a 30.8% inhibition with a corresponding mycelial growth of 61.8 mm, demonstrating substantial efficacy even at reduced dosages. These findings align with the observations of Patel *et al.* [68], who reported that chitosan nanoparticles enhance the sustained release and targeted delivery of agrochemicals, resulting in improved efficacy at lower concentrations.

The significant difference in performance between the two formulations underlines the potential of nanotechnology in enhancing fungicide efficacy. Several studies, including those by Verma *et al.* [85] and Dwivedi *et al.* [19] highlighted the advantages of nanoparticle-based formulations, such as improved solubility, stability, and controlled release, which contribute to their superior performance compared to conventional products. Moreover, the ability of chitosan NPs to maintain efficacy at lower concentrations suggests a potential reduction in chemical input, aligning with sustainable agricultural practices. According to Jiang *et al.* [37], nanoparticle-based formulations not only improve antifungal efficacy but also reduce environmental risks by minimizing chemical runoff and non-target effects.

The enhanced efficacy of the chitosan NP formulation at lower concentrations presents a promising solution for sustainable management of rice blast disease. By reducing the required dosage of hexaconazole, this formulation can lower production costs and minimize environmental impact, as emphasized by Kaur *et al.* [38]. Additionally, its prolonged efficacy at reduced concentrations aligns with integrated pest management strategies aimed at reducing reliance on chemical fungicides.

Fixation of Effective Concentration of Hexaconazole and Hexaconazole Encapsulated in Chitosan NPs (HECNPs)

The effective concentration (EC_{50}) of commercial hexaconazole and HECNPs for inhibiting 50% growth of *P. oryzae* was determined using probit analysis. This analysis was based on the percentage inhibition of mycelial growth observed at varying concentrations *i.e.* 2000 ppm, 1500 ppm, 1000 ppm, 500 ppm, 250 ppm, and 125 ppm. The EC_{50} value for

hexaconazole was calculated as 769 ppm (Fig. 3), while the EC_{50} value for the HECNPs formulation was 194 ppm (Table 2; Fig. 4). Based on the obtained EC_{50} values, subsequent experiments were conducted using 800 ppm of hexaconazole and 200 ppm of HECNPs.

Table 2
Determination of EC_{50} for commercial Hexaconazole and HECNPs against *P. oryzae* by probit analysis

S.No.	Concentration (ppm)	Commercial Hexaconazole			HECNPs		
		LOG of Concentration (X)	Inhibition (%)	Probit values (Y)	LOG of Concentration (X)	Inhibition (%)	Probit values (Y)
1	2000	3.301	100.0	5.674	3.301	100.0	6.269
2	1500	3.176	100.0	5.674	3.176	100.0	5.674
3	1000	3.000	100.0	5.674	3.000	100.0	5.674
4	500	2.699	44.2	4.853	2.699	89.8	5.674
5	250	2.398	7.8	3.580	2.398	73.4	5.624
6	125	2.097	1.9	2.935	2.097	30.8	4.499
-	-	-	Intercept	2.18932	-	-	3.607614
-	-	-	X Variable 1	2.490987	-	-	0.705927

The determination of effective concentaration (EC_{50}) values for hexaconazole and HECNPs provides critical insights into their relative efficacy and potential application in fungal disease management. Using probit analysis, the EC_{50} values for inhibiting 50% of *P. oryzae* growth were calculated as 769 ppm for hexaconazole and 194 ppm for the chitosan NP-encapsulated formulation. These results highlight the enhanced potency of the nanoparticle formulation, offering significant implications for reducing chemical usage in sustainable agriculture.

The EC_{50} value of 769 ppm for the commercial hexaconazole formulation reflects its effective dose requirement to inhibit fungal growth. This value is consistent with findings reported by Patel *et al.* [68], who observed similar concentration-dependent efficacy in conventional triazole fungicides. However, the relatively high EC_{50} value suggests that higher concentrations are necessary to achieve effective fungal control, which may contribute to environmental and economic concerns [30].

In contrast, the HECNPs formulation demonstrated a markedly lower EC_{50} value of 194 ppm, highlighting its superior efficacy in inhibiting fungal growth. The reduced EC_{50} value aligns with the earlier studies which emphasize the role of nanoparticle-based formulations in enhancing the bioavailability and targeted delivery of active ingredients [19, 85]. This substantial reduction in the effective dose underscores the potential of nanotechnology to minimize chemical inputs while maintaining or even improving fungicidal performance.

The enhanced efficacy of the HECNPs formulation is corroborated by existing literature. For instance, Jafernik *et al.* [36] reported that nanoparticle encapsulation of fungicides significantly lowers the EC_{50} values by improving the solubility and controlled release of active compounds. Similarly, Verma *et al.* [86] demonstrated that chitosan-based nanoparticles enhance the interaction of fungicides with fungal cell membranes, leading to more effective inhibition at lower concentrations. The significant difference in EC_{50} values between the two formulations in the present study also reflects the potential of chitosan NPs to address limitations associated with conventional fungicides. By reducing the required dosage, nanoparticle formulations can mitigate environmental risks, decrease production costs, and lower the likelihood of resistance development [19, 38].

Based on the calculated EC_{50} values, subsequent experiments were conducted using 800 ppm of hexaconazole and 200 ppm of HECNPs. These concentrations represent practical dosages for field application, with the nanoparticle formulation requiring a significantly lower amount to achieve comparable efficacy. The results of these experiments could provide further insights into the practical advantages of using nanoparticle-based formulations, particularly in terms of reduced environmental impact and cost-effectiveness.

Characterization of Hexaconazole Encapsulated in Chitosan Nano Particles (HECNPs)

The impregnation of hexaconazole into the chitosan nano particle matrices was confirmed and characterized by using advanced analytical techniques *viz.*, Energy dispersive X-ray spectroscopy, Scanning electron microscopy, Fourier transform infrared spectroscopy, Hydrodynamic diameter measurement and Zeta potential estimation. The hexaconazole concentration was determined by using Gas chromatography- Mass spectrometry.

Energy Dispersive X-ray Spectroscopy (EDS) Analysis of HECNPs

To confirm the chemical composition of the synthesized chitosan nanoparticles encapsulating hexaconazole (HECNPs), Energy Dispersive Spectroscopy (EDS) analysis was conducted. The analysis revealed the presence of carbon (C), oxygen (O), nitrogen (N), and chlorine (Cl) elements in the sample, which align with the chemical structures of both chitosan ($C_{12}H_{24}N_2O_9$) and hexaconazole ($C_{14}H_{17}Cl_2N_3O$). These findings validate the successful encapsulation of hexaconazole within the chitosan nanoparticles (Fig. 5).

The detection of carbon and oxygen highlights the contribution of the chitosan polymer, which consists of a polysaccharide backbone primarily composed of these elements. Nitrogen, a significant component of the amino groups in chitosan, confirms the integrity of the chitosan matrix in the synthesized nanoparticles. The presence of chlorine, a unique element in the molecular structure of hexaconazole, serves as definitive evidence of its incorporation into the chitosan nanoparticles. The simultaneous detection of these elements strongly indicates successful chemical interaction and encapsulation of hexaconazole within the chitosan nanoparticles.

These findings emphasize the effectiveness of the encapsulation process and demonstrate that the synthesized nanoparticles retained the chemical signatures of both chitosan and hexaconazole. Furthermore, the EDS analysis confirms the reliability of the synthesis methodology and the stability of the chemical composition in the prepared HECNPs. This confirmation is pivotal for future studies exploring the functional properties and application potential of HECNPs as agrochemical formulations.

Similar results have been observed in recent studies, where EDS analysis has been used to verify the chemical composition of nanoparticles encapsulating bioactive compounds. For example, curcumin [15, 55] and meloxicam [92] loaded chitosan nanoparticles were successfully characterized using EDS, identifying elemental peaks corresponding to both the polymer and the encapsulated compound. Likewise, Zhao *et al.* [98] demonstrated the efficacy of chitosan as an encapsulation material, showing distinct elemental signatures for both the polymer and encapsulated drug using EDS analysis.

The confirmation of hexaconazole encapsulation through EDS is critical as it ensures the successful synthesis of functional nanoparticles for potential agricultural applications. Chitosan nanoparticles have been widely recognized for their biocompatibility, biodegradability, and ability to enhance the solubility and stability of encapsulated hydrophobic compounds [50]. Encapsulating hexaconazole in chitosan nanoparticles not only ensures its controlled release but also mitigates the environmental toxicity associated with conventional fungicide delivery systems.

Additionally, the results support the hypothesis that electrostatic interactions between the amine groups in chitosan and the functional groups in hexaconazole play a vital role in the encapsulation process. This observation emphasized the importance of electrostatic interactions in synthesizing polymeric nanoparticles for encapsulating hydrophobic compounds [39]. Thus, the EDS analysis further provides definitive evidence of the successful synthesis of hexaconazole-encapsulated

chitosan nanoparticles by confirming the presence of key elemental components. The results are in agreement with previous studies, underscoring the potential of chitosan nanoparticles as efficient delivery systems for agrochemicals.

Hydrodynamic Diameter and Zeta Potential of HECNPs

The size distribution of HECNPs was measured using dynamic light scattering (DLS) in a medium of 0.1% carboxy methyl cellulose (CMC). The hydrodynamic diameter of the HECNPs was found to be 92.8 nm, indicating a nanoscale size range suitable for potential agrochemical applications (Fig. 6). The use of CMC as a dispersion medium ensures that the nanoparticles remain stably suspended, reducing the likelihood of aggregation during the analysis.

The zeta potential, a key indicator of colloidal stability, was determined to be + 31.2 mV for the HECNPs (Fig. 7). Zeta potential reflects the surface charge of particles, which directly impacts the stability of colloidal dispersions. Particles with a zeta potential greater than + 30 mV or less than − 30 mV typically exhibit sufficient electrostatic repulsion to prevent aggregation, thereby maintaining colloidal stability [34]. In a similar study, Yegireddy *et al.* [92] observed the zeta potential of + 39.9 mV with hydrodynamic diameter of 138.5 nm of chitosan encapsulated meloxicam nano particles. The positive zeta potential value in this study is attributed to the presence of free amine groups on the polymer's surface, which confer a positive charge to the nanoparticles. Similar findings have been reported for chitosan-based nanoparticles in previous studies, where the presence of amine groups contributed to a positive zeta potential [21, 74, 97].

The measured zeta potential of HECNPs in this study is comparable to values reported in the literature for other chitosan-based nanoparticles, confirming the consistency of these materials' surface characteristics. For example, Zhang *et al.* [97] reported zeta potentials in the range of + 30 mV to + 50 mV for chitosan nanoparticles prepared under various conditions. Similarly, Rajashekaraiah *et al.* [74] observed positive zeta potential values for chitosan nanoparticles, which were attributed to the protonation of amino groups under acidic conditions.

The hydrodynamic diameter and zeta potential of HECNPs suggest that these nanoparticles possess favourable colloidal stability and surface charge characteristics for potential agricultural applications. The nanoscale size enables efficient interaction with biological systems, while the positive zeta potential can facilitate interactions with negatively charged biomolecules or cell membranes.

Fourier Transform Infrared (FT-IR) Spectroscopy of HECNPs

The Fourier Transform Infrared (FT-IR) spectroscopy analysis of chitosan nanoparticles and encapsulated composite are presented in the superimposed graph. A comparative analysis of the spectral changes provides critical insights into the molecular interactions and structural integrity of chitosan nanoparticles, encapsulated composite containing hexaconazole.

Chitosan nanoparticles exhibit distinct spectral features in their FT-IR spectrum, which are indicative of their chemical structure. A broad absorption band in the range of 3200–3500 cm^{-1} corresponds to O-H and N-H stretching vibrations, confirming the presence of hydroxyl and amine groups inherent to chitosan (Table 3). Furthermore, peaks at 1640 cm^{-1} and 1560 cm^{-1} are associated with amide I (C = O stretching) and amide II (N-H bending) vibrations, respectively, affirming the presence of amide linkages within the chitosan framework. Additionally, the band observed at 1020–1100 cm^{-1} reflects C-O-C stretching vibrations associated with glycosidic linkages, thereby reinforcing the polysaccharide backbone of chitosan. Recent studies demonstrate the significance of these functional groups in augmenting the hydrophilicity and bioactivity of chitosan nanoparticles [33, 72].

Table 3
FT-IR spectra of chitosan nanoparticles

S.No	Absorption (Cm^{-1})	Bonding Nature	Functional groups	Intensity
1	525	C-I stretch	Aliphatic organo halogen compounds	Weak, sharp
2	700	$-(CH_2)_n-$ stretch	Methylene	Weak, sharp
3	825	C-H bend	Aromatic ring	Weak, Sharp
4	970	P-O-C- stretch (aromatic)	Hetero-oxy compounds	Medium, Sharp
5	1100	C-N stretch	Amine	Strong, sharp
6	1275	Aryl-O stretch	Ether and Oxy compounds	Weak, sharp
7	1400	O-H stretch S = O stretch	Alcohol, Sulphate	Strong, Sharp
8	1575	N-O stretch	Hetero-oxy compounds	Strong, sharp
9	1700	C = O stretch	Amide I	Medium, Sharp
10	2845	C-H stretch	Methylene	Strong, Sharp
11	2925	C-H stretch	2-Butanone	Strong, sharp
12	3400	O-H stretch	Ethanol	Medium, Broad

The encapsulated composite of hexaconazole exhibits a distinctive spectral profile, characterized by significant absorptions in the 1600–1700 cm^{-1} range, which correspond to C = N and aromatic C = C stretching vibrations. This aligns with recent findings, regarding the spectral characteristics of triazole fungicides, emphasizing the importance of these peaks in identifying the chemical structure of hexaconazole (Table 4 and Fig. 8) [18]. In addition, the observed C-O stretching vibrations in the 1200–1300 cm^{-1} range and C-H out-of-plane bending vibrations around 800–900 cm^{-1} reflect the aromatic and functional diversity present in the compound. Notably, the broad O-H and N-H band observed between 3200–3500 cm^{-1} demonstrates a shift to lower wavenumbers, indicative of hydrogen bonding interactions between chitosan and hexaconazole, thereby enhancing compatibility and stability within the composite [43]. Furthermore, the presence of a C-Cl stretch at approximately 725 cm^{-1} corroborates the integration of hexaconazole, while shifts in the amide I and II peaks suggest electrostatic interactions with the amino groups of chitosan [10]. The reductions in intensity and minor shifts of the C = N and aromatic C = C stretching vibrations confirm successful encapsulation without compromising the structural integrity of hexaconazole, while the sustained prominence of C-O-C stretching vibrations at 1020–1100 cm^{-1} illustrates the stability of the chitosan backbone, a crucial factor in its role as a carrier material.

Table 4
FT-IR spectra of HECNPs

S.No	Absorption (Cm^{-1})	Bonding Nature	Functional groups	Intensity
1	525	C-I stretch	Aliphatic organo halogen compounds	Strong, Sharp
2	625	C-I stretch	Aliphatic organo halogen compounds	Weak, Sharp
3	725	C-Cl stretch	Aliphatic organo halogen compounds	Strong, Sharp
4	850	C-O-O- stretch	Ether and oxy compound	Strong, Sharp
5	925	P-O- C stretch	Hetero oxy compound	Medium, Sharp
6	1100	C-N stretch	Amine	Strong, Sharp
7	1200	C-N stretch	Tertiary Amino Compound	Strong, Sharp
8	1350	P = O stretch	Phosphorous oxy compound	Strong, Sharp
9	1400	O-H stretch S = O stretch	Alcohol,Sulphate	Weak, Sharp
10	1510	C = C-C stretch	Aromatic ring (aryl)	Weak, Sharp
11	1625	C = C stretch	Olefinic (alkene)	Strong, Sharp
12	1700	C = O stretch	Amide I	Strong, Sharp
13	2600	S-H stretch	Thiols	Weak, Broad
14	2870	O-H stretch	Carboxylic acid	Strong, Sharp
15	2925	C-H stretch	Methylene	Strong, Sharp
16	3290	O-H stretch	Alcohol & hydroxylcompound	Medium, Broad
17	3450	N-H stretch	Heterocyclic amine	Strong, Broad

The FT-IR analysis provides compelling evidence for the successful encapsulation of hexaconazole within chitosan nanoparticles. Notable spectral shifts and diminished intensities in the distinct peaks signify the occurrence of interactions, chiefly hydrogen bonding and electrostatic forces, between hexaconazole and chitosan. This encapsulation not only enhances the functional characteristics of the chitosan nanoparticles, rendering them adept carriers for the controlled release of hexaconazole in agricultural contexts, but it also stabilizes the active compound, thereby prolonging its efficacy and potentially mitigating environmental impacts, as discussed in recent research on nanoparticle delivery systems [13, 44, 94]. The combined bioactivity of chitosan with the fungicidal properties of hexaconazole creates a promising framework for targeted delivery, ultimately addressing critical issues in modern agricultural practices. Future investigations should focus on the scalability of this encapsulation technique and its practical implications in field applications, aiming to enhance both performance and cost-effectiveness in agricultural settings.

Scanning Electron Microscopy (SEM) Analysis of HECNPs

The surface morphology and size distribution of HECNPs were analyzed using Scanning Electron Microscopy (SEM). The SEM micrographs revealed that the HECNPs exhibited a shape ranging from round to cuboidal with a size distribution between 90 and 120 nm (Fig. 9). These observations confirm the uniformity in the morphology and size of the synthesized nanoparticles, which is critical for their functional performance in agrochemical applications.

The observed size range aligns with the reported dimensions of chitosan nanoparticles in previous studies, indicating the suitability of the synthesis methodology. For instance, similar size distribution of meloxicam-loaded (110–200 nm) [92] and curcumin-loaded (80–140 nm) [2] chitosan nanoparticles synthesized was reported using ionic gelation techniques. Such nanoscale sizes are advantageous as they improve the surface area-to-volume ratio, facilitating better interaction with the target sites and enhancing the bioavailability of the encapsulated compound.

The round to cuboidal morphology observed in HECNPs can be attributed to the influence of the encapsulated hexaconazole, as the molecular structure and encapsulation conditions can significantly affect nanoparticle shape. Earlier studies demonstrated that the shape of chitosan nanoparticles can vary depending on the nature of the encapsulated compound, with cuboidal shapes often linked to the encapsulation of hydrophobic molecules like hexaconazole [8, 82].

The size and morphology of nanoparticles are crucial factors influencing their stability, drug release kinetics, and bioactivity. The 90–150 nm size range of HECNPs suggests their potential for effective delivery, as nanoparticles of this size can easily penetrate biological barriers, enhancing the controlled release of hexaconazole. Similar findings were reported by Sharma *et al.* [80] and Poshina *et al.* [70], who emphasized the role of nanosized chitosan carriers in improving the solubility and bioavailability of hydrophobic agrochemicals. Furthermore, the morphology observed in this study is consistent with Marin-Silva *et al.* [48] who noted that cuboidal shapes in chitosan nanoparticles can enhance structural stability and reduce aggregation, thereby improving their performance as delivery vehicles.

Gas Chromatography Mass Spectrometry Analysis

The analysis was conducted using the Multiple Reaction Monitoring (MRM) mode in GC-MS, where hexaconazole concentration was identified based on its retention times, along with target and qualifier ions. Quantitation was determined by calculating the peak area ratio of the targets relative to an internal standard.

For method validation, calibration curves for hexaconazole were prepared at five concentrations ranging from 0.01 to 0.1 µg/mL, yielding a linear response with the equation Y = 16.21457X − 45.01181 and a correlation coefficient (R^2) of 0.999, indicating excellent linearity. Repeatability was assessed through six injections of standard solutions at concentrations of 0.01 µg/mL and 0.1 µg/mL, confirming the precision of the method. Recovery studies revealed hexaconazole concentrations of 10.85 ppb, 20.33 ppb, 29.41 ppb, 48.74 ppb, and 100.65 ppb when spiked at levels of 0.01, 0.02, 0.03, 0.05, and 0.1 µg/mL, respectively. The retention time for hexaconazole was recorded at 11.45 minutes, with the chromatogram of hexaconazole spiked in the nano formulation illustrated in Fig. 10. Recovery experiments, performed to validate the extraction method, involved control samples fortified at five concentration levels (0.01 to 0.1 µg/mL), yielding a relative standard deviation (RSD) of 6.96%, thus demonstrating the precision and accuracy of the standardized method for determining hexaconazole concentrations [65].

Hexaconazole concentrations in HECNPs were determined by diluting the prepared nanoparticles in proportions of 1:5, 1:10, 1:15, and 1:20 with HPLC-grade water, followed by GC-MS analysis. The measured concentrations for these dilutions were 5008.6 ppm, 1001.5 ppm, 202 ppm, and 39.75 ppm, respectively. Each spiked concentration was analyzed in four replicates, with a mean standard deviation below 8.72%, indicating high reproducibility [12]. Based on *in-vitro* evaluation, the EC_{50} value of HECNPs was determined to be 200 ppm, making the 1:15 dilution suitable for field experiments.

Residue analysis of hexaconazole in paddy leaves was performed to study its dissipation in rice plants sprayed with either commercial hexaconazole (800 ppm) or HECNPs (200 ppm). Residue concentrations were analyzed using GC-MS at four intervals: 0 days (immediately after spraying), 5 days, 10 days, and 15 days. Both formulations showed a decline in hexaconazole residues over time but were detectable up to 15 days post-application. In rice plants treated with the commercial formulation, residue concentrations decreased from 800.6 ppm at 0 days to 8.0 ppm at 15 days (Table 5 and Fig. 11). Similarly, in plants treated with HECNPs, concentrations declined from 200.6 ppm at 0 days to 15 ppm at 15 days. Each sampling interval was replicated four times to ensure precision. When analysed using Tukey's test at $p = 0.05$ (95%

confidence level), there exists significant difference among the concentrations of the fungicides obtained at different days of spraying with the least significant difference of 74.68 for commercial hexaconazole-treated plants and 12.65 for HECNPs-treated plants. These findings demonstrate that the nanoformulation (HECNPs) exhibited improved dissipation dynamics and reduced residue persistence compared to the commercial formulation.

Table 5
Determination of hexaconazole concentration in paddy leaves

Days after spraying	Commercial formulation		HECNPs	
	Concentration (ppm)	Standard Deviation	Concentration (ppm)	Standard Deviation
0 days	802.6[a]	3.3	200.6[a]	4.4
5 days	471.0[b]	70.6	115.6[b]	3.2
10 days	115.5[c]	7.5	78.6[c]	8.4
15 days	8.0[d]	2.1	15.0[d]	6.4
SE(m) (±)	17.7	-	3.0	-
CD (P ≤ 0.01)	55.4	-	9.3	-
CV (%)	10.1	-	5.8	-

The method validation for determining hexaconazole concentrations demonstrated a robust and reliable analytical approach, showcasing excellent linearity across the calibration range (0.01–0.1 µg/mL) with a correlation coefficient (R^2) of 0.999. This high linearity confirms the method's capability to accurately quantify hexaconazole, aligning with established pesticide residue analysis studies [29]. Repeatability assessments, with low standard deviations at multiple concentration levels, further underscored the precision of the method, while the consistent retention time (11.45 minutes) validated the reliability of chromatographic conditions.

The recovery experiments provided additional evidence of method accuracy, achieving recoveries ranging from 10.85 ppb to 100.65 ppb with a relative standard deviation (RSD) of 6.96%. These results are comparable to other studies on pesticide residue analysis, which highlight the method’s suitability for quantifying fungicides in complex matrices [67, 96]. The ability to maintain a low RSD across a wide range of concentrations emphasizes the utility of this method for routine monitoring in agricultural and environmental contexts.

In the analysis of hexaconazole concentrations in HECNPs, the method exhibited high reproducibility. Dilution experiments with HECNPs (1:5, 1:10, 1:15, and 1:20) revealed hexaconazole concentrations of 5008.6 ppm, 1001.5 ppm, 202.0 ppm, and 39.75 ppm, respectively, with low mean standard deviations (< 8.72%) across replicates. These findings align with validated methodologies for nanopesticides, reinforcing the method's reliability [93]. The determination of an EC_{50} value of 200 ppm for HECNPs supports their potential agricultural application, with the 1:15 dilution emerging as the most suitable for field experiments, balancing efficacy and environmental safety.

The dissipation study of hexaconazole residues in paddy leaves highlighted the comparative advantages of nanoformulations. Both the commercial formulation (800 ppm) and the nanoformulation (200 ppm) showed declining residue levels over 15 days, but the nanoformulation exhibited significantly improved dissipation dynamics. Residue concentrations in the nanoformulation-treated plants decreased from 200.6 ppm on day 0 to 15 ppm by day 15, while the commercial formulation declined from 2000 ppm to 10.3 ppm over the same period. These results demonstrate the potential of nanopesticides to enhance efficacy while minimizing environmental impact [95].

Statistical analysis using Tukey's test at $p = 0.05$ further validated the superior performance of HECNPs. The least significant difference (LSD) values of 74.68 for the commercial formulation and 12.65 for the nanoformulation-treated plants underscore the enhanced precision of the nanoformulation. Similar studies have shown that nanopesticides effectively balance pest control with reduced residue persistence, mitigating environmental contamination risks [66].

Recent advancements in analytical techniques have significantly contributed to fungicide residue analysis. Gas chromatography-mass spectrometry (GC-MS) remains a cornerstone in pesticide residue monitoring due to its sensitivity, specificity and versatility. The method's ability to maintain accuracy in the presence of matrix interferences, supported by techniques such as matrix-matched calibration, has been critical in addressing challenges posed by complex plant matrices [24]. Moreover, the adoption of advanced sample preparation techniques, such as QuEChERS, has streamlined the extraction of fungicide residues, enhancing recovery rates and analysis efficiency [6, 47].

The integration of nanoformulations with validated analytical methods represents a significant step forward in agricultural practices. By reducing residue persistence and environmental impact, nanopesticides like HECNPs offer a sustainable alternative to conventional formulations. The findings of this study contribute to the growing body of evidence supporting the use of nanopesticides for effective pest management and environmental protection. Further research is warranted to evaluate the field-level efficacy of HECNPs in managing plant diseases and thereby ensuring food security.

TESTING THE FIELD EFFICACY OF HECNPS IN MANAGING RICE BLAST

The field efficacy of HECNPs in reducing the incidence of rice blast was assessed over two consecutive rabi cropping seasons, 2022-23 (season 1) and 2023-24 (season 2). To assess the accuracy of the results obtained during the rabi season of 2022-23, the treatments were applied in both the Uniform Blast Nursery (UBN) and the field during the rabi season of 2023-24. Commercial hexaconazole served as the control to compare the effectiveness of the HECNP treatments. Additionally, chitosan nanoparticles without hexaconazole were included in the study to evaluate the standalone efficacy of chitosan nanoparticles. Both the incidence of the disease and yield attributes were recorded. The findings from the study are summarized below.

Disease incidence

In season 1, the highest disease incidence of 94.8% was recorded in untreated control plots (T9), highlighting the severity of the disease in the absence of treatment. The treatment with HECNPs at 12.5 g a.i. ha^{-1} with two sprays (T6) and one spray (T5) achieved the lowest leaf blast incidence, with 26.6% and 31.8%, respectively. These treatments resulted in disease reduction efficiencies of 66.9% and 60.2% over control and AUDPC values of 110.5 and 282.5, respectively. Following these, treatments T4, T3, and T2 exhibited disease incidences of 35.5%, 38.5%, and 40.0%, with reduction efficiencies of 55.5%, 52.0%, and 50.3% over control, and corresponding AUDPC values of 464.5, 614.2, and 750.0. The treatments with HECNPs applied at 2.5 g a.i. ha^{-1} with a single spray (T1) and commercial hexaconazole applied at 20 g a.i. ha^{-1} (T7) demonstrated statistically similar results. They showed disease incidences of 44.4% and 49.6%, with reduction efficiencies of 44.9% and 38.0% over control, and AUDPC values of 867.0 and 1100.5, respectively. On the other hand, chitosan applied at 2.0 g L^{-1} (T8) resulted in a statistically distinct disease incidence of 54.0%, with a reduction efficiency of 32.1% and an AUDPC value of 1278.0 (Table 6). The untreated control (T9) recorded the highest disease incidence of 80.7%, with an AUDPC value of 1407.0, thus, highlighting the severity of disease progression without intervention.

Table 6
Efficacy of HECNPs in rice blast management under field conditions - disease index

S.No.	Treatment	*First Season	*Second Season	*UBN	% reduction over control			Pooled	AUDPC	
					Season1	Season 2	UBN	#Season 1 x Season 2	Season 1	Season 2
1	T1: HECNPs @ 2.5 g a.i. ha^{-1} (1 spray)	44.4^{de} (6.7)	52.5^{cde} (7.3)	48.9^{cd} (7.0)	44.9	37.0	48.4	48.5^{e} (11.4)	867.0	904.5
2	T2: HECNPs @ 2.5 g a.i. ha^{-1} (2 sprays)	40.0^{cd} (6.4)	46.6^{cde} (6.8)	43.0^{bcd} (6.5)	50.3	43.9	54.6	43.3^{d} (10.6)	750.0	795.5
3	T3: HECNPs @ 5.0 g a.i. ha^{-1} (1 spray)	38.5^{bcd} (6.2)	41.4^{bcd} (6.4)	38.5^{bcd} (6.2)	52.0	49.7	59.3	40.0^{cd} (10.0)	614.2	642.0
4	T4: HECNPs @ 5.0 g a.i. ha^{-1} (2 sprays)	35.5^{bc} (6.0)	38.5^{bc} (6.2)	32.6^{abc} (5.7)	55.5	53.7	65.6	37.0^{c} (9.8)	464.5	495.0
5	T5: HECNPs @ 12.5 g a.i. ha^{-1} (1 spray)	31.8^{ab} (5.7)	29.6^{ab} (5.5)	25.9^{ab} (5.0)	60.2	64.4	72.6	30.7^{b} (8.8)	282.5	293.5
6	T6: HECNPs @ 12.5 g a.i. ha^{-1} (2 sprays)	26.6^{a} (5.2)	23.7^{a} (4.9)	18.5^{a} (4.3)	66.9	71.5	80.4	25.1^{a} (7.8)	110.5	122.0
7	T7: Hexaconazole @ 20.0 g a.i. ha^{-1}	49.6^{ef} (7.1)	55.5^{de} (7.5)	54.8^{d} (7.4)	38.0	33.7	42.1	52.5^{f} (12.2)	1100.5	1152.0
8	T8: Chitosan @ 2.0 g L^{-1}	54.0^{f} (7.4)	61.4^{e} (7.9)	59.3^{d} (7.7)	32.1	26.4	37.5	57.7^{g} (13.0)	1278.0	1307.0
9	T9: Untreated Control	80.7^{g} (9.0)	83.7^{f} (9.2)	94.8^{e} (9.7)	-	-	-	82.2^{h} (17.0)	1407.0	1487.0
	SE(m) (±)	0.20	0.34	0.47	-	-	-	-	-	-
	C.D. (P ≤ 0.01)	0.62	1.03	1.43	-	-	-	-	-	-
	C.V.(%)	5.35	8.57	12.35	-	-	-	-	-	-

*values in the parenthesis are Arc sin transformed; #values in the parenthesis are Atkins transformed

In season 2 (main field), the treatment with HECNPs at 12.5 g a.i. ha^{-1} with two sprays (T6) and one spray (T5) achieved the lowest leaf blast incidences of 23.7% and 29.6%, respectively, with reductions of 71.5% and 64.4% over the untreated control. The corresponding AUDPC values were 122.0 and 293.5, respectively. These were followed by treatments T4 and T3, which recorded disease incidences of 38.5% and 41.4%, achieving reduction efficiencies of 53.7% and 49.7% over control, with AUDPC values of 495.0 and 642.0, respectively. The treatments with HECNPs at 2.5 g a.i. ha^{-1}(T1 and T2), commercial hexaconazole at 20.0 g a.i. ha^{-1} (T7), and chitosan at 2.0 g L^{-1} (T8) showed statistically similar results, with disease incidences of 46.6%, 52.5%, 55.5%, and 61.4%, respectively. These treatments achieved disease reductions of 43.9%, 37.0%, 33.7%, and 26.4% over the control, with corresponding AUDPC values of 795.5, 904.5, 1152.0, and 1307.0.

To comprehensively evaluate the efficacy of HECNPs against rice blast incidence on seedlings, a separate experiment was conducted in UBN using the same treatments. In season 2 (UBN), the significantly lowest disease incidences were observed in plots treated with HECNPs at 12.5 g a.i. ha^{-1} with two sprays (T6), one spray (T5), and HECNPs at 5.0 g a.i. ha^{-1} with two sprays (T4), with disease incidences of 18.5%, 25.9%, and 32.6%, respectively. These treatments achieved disease reductions of 80.4%, 72.6%, and 65.6% over the untreated control. Following these, plots treated with one spray of HECNPs at 5.0 g a.i. ha^{-1}(T3) and HECNPs at 2.5 g a.i. ha^{-1} with two sprays (T2) and one spray (T1) showed disease incidences of 38.5%, 43.0%, and 48.9%, respectively. The disease incidences recorded for commercial hexaconazole applied at 20.0 g a.i. ha^{-1} (T7) and chitosan applied at 2.0 g L^{-1} (T8) were 54.8% and 59.3%, which were statistically similar, with disease reduction efficiencies of 42.1% and 37.5%, respectively.

Pooled analysis

The interaction study, which pooled disease incidences from both season 1 and season 2 in the main plots, revealed a significantly lowest disease incidence of 25.1% in plots treated with HECNPs at 12.5 g a.i. ha^{-1} with two sprays (T6). This was followed by plots treated with HECNPs at 12.5 g a.i. ha^{-1} with one spray (T5), which recorded a disease incidence of 30.7%. The plots treated with HECNPs at 5.0 g a.i. ha^{-1} (T3 and T4) showed similar results, with disease incidences of 40.0% and 37.0%, respectively. In contrast, significantly higher disease incidences of 52.5% and 57.7% were observed in plots treated with commercial hexaconazole (T7) and chitosan (T8), respectively. However, the disease incidences for T7 and T8 were statistically on par across both the seasons.

The findings of this study underscore the significant potential of HECNPs as an innovative and sustainable alternative to conventional fungicides for managing rice blast disease. The consistent performance of HECNP treatments across the two cropping seasons and experimental conditions highlights their reliability, efficacy, and adaptability to varying environmental challenges. HECNPs at 12.5 g a.i. ha^{-1} with two sprays (T6) demonstrated the most substantial disease reduction, with incidences reduced to 26.6% and 23.7% in seasons 1 and 2, respectively, alongside disease reduction efficiency of 66.9% and 71.5%. These results highlight the capacity of HECNPs to significantly lower disease severity and surpass the efficacy of commercial hexaconazole. The consistent reduction in AUDPC values across seasons further reinforces the robust disease management potential of this nanoparticle formulation. The findings align with previous studies demonstrating the enhanced bioavailability and controlled release properties of nanocarriers in improving fungicide efficiency [14, 81].

Even with a single spray (T5), HECNPs at 12.5 g a.i. ha^{-1} were effective in reducing disease incidence, achieving 31.8% and 29.6% reductions in seasons 1 and 2, respectively. This observation is particularly noteworthy as it suggests that reducing the frequency of fungicide application is feasible without compromising efficacy, supporting the movement toward more sustainable agricultural practices. The effectiveness of HECNPs at lower concentrations (5.0 g a.i. ha^{-1}) further emphasizes the potential of nanoparticle formulations to achieve comparable results with reduced chemical inputs. This corroborates findings by Shah *et al.* [79], which highlighted the enhanced bio-efficacy of nanocarrier-based delivery systems. Such an approach addresses concerns related to the overuse of fungicides, including environmental pollution and the risk of pathogen resistance development. The standalone application of chitosan nanoparticles (T8) achieved moderate disease reduction efficiencies of 32.1% and 26.4% in seasons 1 and 2, respectively. Similarly, moringa-chitosan nanoparticles

demonstrated a significant reduction in rice blast incidence, achieving a 77.7% reduction [31]. While the antifungal and elicitor properties of chitosan played a role in disease control, the findings suggest that combining chitosan with an active fungicide, such as hexaconazole, is essential for maximizing its efficacy [32]. This underscores the synergistic potential of integrating chitosan with fungicides to achieve more effective disease management.

The UBN experiments in season 2 provided valuable insights into the performance of HECNPs under high disease pressure. Treatments foliar spray of HECNPs at 12.5 g a.i. ha^{-1}, two sprays (T6) and one spray (T5) consistently demonstrated superior disease reduction efficiencies, mirroring results was observed in the main field trials. This robustness under adverse conditions underscores the potential of HECNPs to provide reliable disease management solutions in diverse agro-climatic environments. The consistency of these findings emphasize the ability of nanoparticle formulations to enhance resistance even under severe disease pressure [1].

Commercial hexaconazole (T7) exhibited moderate efficacy in reducing disease incidence, yet its performance was consistently inferior to HECNP treatments. The superior results of nanoparticle-based formulations especially prepared by encapsulating in silica, zinc oxide and chitosan are attributed to their controlled release properties, enhanced penetration, and increased bioavailability, as documented in prior studies [26, 45, 73, 91]. These advantages position HECNPs as a promising alternative for integrated pest management strategies aimed at improving crop health while reducing environmental impact. Nanoparticle-based fungicides not only enhance efficacy but also align with the goals of sustainable agriculture by minimizing chemical inputs and reducing environmental toxicity. For instance, treatments like HECNPs at 5.0 g a.i. ha^{-1} demonstrate that effective disease management can be achieved with reduced active ingredient concentrations, paving the way for eco-friendly solutions to address rice blast disease.

Yield attributes

Treatments with higher concentrations of HECNPs and multiple spray applications consistently resulted in significantly higher rice yields across both seasons. Among the tested treatments, HECNPs @ 12.5 g a.i. ha^{-1} with 2 sprays (T6) produced the highest yields, achieving 3250 kg/ha in season 1 and 3083.3 kg/ha in season 2, significantly outperforming all other treatments and controls, including the commercial hexaconazole (T7) and chitosan (T8). Following T6, HECNPs @ 12.5 g a.i. ha^{-1} with 1 spray (T5) recorded yields of 2833.3 kg/ha in season 1 and 2750.0 kg/ha in season 2, while HECNPs @ 5.0 g a.i. ha^{-1} with 2 sprays (T4) yielded 2500.0 kg/ha in season 1 and 2416.6 kg/ha in season 2. The standard chemical treatment, hexaconazole @ 20.0 g a.i. ha^{-1} (T7), showed moderate efficacy with yields of 1750 kg/ha in season 1 and 1833.3 kg/ha in season 2. Similarly, the alternative treatment, chitosan @ 2.0 g L^{-1} (T8), produced yields of 1583.3 kg/ha in both seasons, comparable to the untreated control. The untreated control (T9) exhibited the lowest productivity, with yields of 1333.3 kg/ha in season 1 and 1250.0 kg/ha in season 2 (Table 7). These results clearly demonstrate that higher concentrations of HECNPs, particularly with two spray applications, are highly effective in significantly enhancing rice yield.

Table 7
Efficacy of HECNPs in rice blast management under field conditions – yield per plot

S.No.	Treatments	Yield						NRRI (Rs.)		
		Season 1 (S1)		Season 2 (S2)		S1 X S2		Season 1	Season 2	S1 X S2
		(Kg/ Plot)	Kg/ Hac.	(Kg/ Plot)	Kg/ Hac.	(Kg/ Plot)	Kg/ Hac.			
1	T1: HECNPs @ 2.5 g a.i. ha^{-1} (1 spray)	2.1^{cde}	1750.0	2.0^{cd}	1666.6	2.1^{cd}	1750.0	1.89^{f}	1.83^{f}	1.86^{g}
2	T2: HECNPs @ 2.5 g a.i. ha^{-1} (2 sprays)	2.3^{cde}	1916.6	2.3^{bcd}	1916.6	2.3^{bcd}	1916.6	2.12^{e}	2.10^{e}	2.10^{e}
3	T3: HECNPs @ 5.0 g a.i. ha^{-1} (1 spray)	2.7^{bcd}	2250.0	2.6^{abcd}	2166.6	2.7^{bc}	2250.0	2.53^{d}	2.40^{d}	2.47^{d}
4	T4: HECNPs @ 5.0 g a.i. ha^{-1} (2 sprays)	3.0^{abc}	2500.0	2.9^{abc}	2416.6	2.9^{abc}	2416.6	2.76^{c}	2.66^{c}	2.70^{c}
5	T5: HECNPs @ 12.5 g a.i. ha^{-1} (1 spray)	3.4^{ab}	2833.3	3.3^{ab}	2750.0	3.4^{ab}	2833.3	3.17^{b}	3.13^{b}	3.15^{b}
6	T6: HECNPs @ 12.5 g a.i. ha^{-1} (2 sprays)	3.9^{a}	3250.0	3.7^{a}	3083.3	3.8^{a}	3166.6	3.66^{a}	3.53^{a}	3.59^{a}
7	T7: Hexaconazole @ 20.0 g a.i. ha^{-1}	2.1^{cde}	1750.0	2.2^{bcd}	1833.3	2.2^{cd}	1833.3	1.91^{f}	2.03^{e}	1.97^{f}
8	T8: Chitosan @ 2.0 g L^{-1}	1.9^{de}	1583.3	1.9^{cd}	1583.3	1.9^{cd}	1583.3	1.71^{g}	1.69^{g}	1.69^{h}
9	T9: Untreated Control	1.6^{e}	1333.3	1.5^{d}	1250.0	1.5^{d}	1250.0	1.35^{h}	1.28^{h}	1.31^{i}
	SE(m) (±)	0.29	-	0.38	-	0.36	-	0.03	0.03	0.02
	C.D. ($P \leq 0.01$)	0.89	-	1.15	-	0.12	-	0.11	0.09	0.07
	C.V. (%)	19.91	-	26.24	-	3.64	-	2.76	2.46	2.61

The pooled analysis between the yields obtained in season 1 and season 2 was analyzed by pooling the data from both seasons. The results revealed that HECNPs @ 12.5 g a.i. ha^{-1} with 2 sprays (T6) achieved the highest yield, producing 3166.6 kg/ha. This was followed by HECNPs @ 12.5 g a.i. ha^{-1} with 1 spray (T5) and HECNPs @ 5.0 g a.i. ha^{-1} with 2 sprays (T4), which recorded yields of 2833.3 kg/ha and 2416.6 kg/ha, respectively. The treatments HECNPs @ 2.5 g a.i. ha^{-1} with 1 spray (T1), hexaconazole @ 20.0 g a.i. ha^{-1} (T7) and chitosan @ 2.0 g L^{-1} (T8) exhibited comparable yields of 1750.0 kg/ha, 1833.3 kg/ha, and 1583.3 kg/ha, respectively. In contrast, the untreated controls (T9) produced the lowest yield of 1250.0 kg/ha, significantly lower than all other treatments, emphasizing the importance of proper treatment to maximize rice yield.

These findings clearly demonstrate that higher concentrations of HECNPs, particularly when applied twice, are highly effective in substantially enhancing rice productivity. The study highlights the potential of HECNPs as an innovative and powerful solution for improving rice yields, especially at higher concentrations with multiple spray applications.

Net Returns from the Rupee Invested (NRRI)

The treatment HECNPs @ 12.5 g a.i. ha^{-1}, 2 sprays (T6) recorded the highest NRRI values of 3.66 in season 1 and 3.53 in season 2. This is followed by HECNPs @ 12.5 g a.i. ha^{-1}, 1 spray (T5) with NRRI of 3.17 in season 1 and 3.13 in season 2. The commercial hexaconazole @ 20.0 g a.i. ha^{-1} treated plots (T7) recorded the NRRI of 1.91 in season 1 and 2.03 in season 2. The chitosan treated plots exhibited the NRRI of 1.71 in season 1 and 1.69 in season 2. In contrast, the untreated control (T9) had the lowest NRRI values of 1.35 and 1.28, reflecting the minimal productivity under untreated conditions.

This study provides compelling evidence that treatments with higher concentrations of hexaconazole encapsulated in chitosan nanoparticles (HECNPs) and multiple spray applications significantly enhance rice yields across cropping seasons. Among the tested treatments, HECNPs @ 12.5 g a.i. ha^{-1} with two sprays (T6) achieved the highest productivity, yielding 3.9 kg/plot in season 1 and 3.7 kg/plot in season 2, with a pooled average yield of 3.8 kg/plot. The treatment T6 also demonstrated the highest NRRI values of 3.66 in season 1 and 3.53 in season 2, underscoring its economic superiority. These yields were consistently superior to those of both commercial hexaconazole (T7) and standalone chitosan nanoparticles (T8). HECNPs @ 12.5 g a.i. ha^{-1} with one spray (T5) also demonstrated promising results, producing 3.4 kg/plot in season 1 and 3.3 kg/plot in season 2, with a pooled average yield of 3.4 kg/plot. Similarly, HECNPs @ 5.0 g a.i. ha^{-1} with two sprays (T4) yielded 3.0 kg/plot in season 1 and 2.9 kg/plot in season 2, underscoring the potential of moderate-concentration HECNP formulations to effectively boost rice productivity.

In contrast, commercial hexaconazole @ 20.0 g a.i. ha^{-1} (T7) demonstrated moderate efficacy, yielding 2.1 kg/plot in season 1 and 2.2 kg/plot in season 2. The result obtained indicate that traditional fungicides are less effective due to limited bioavailability and absence of controlled release mechanisms [91]. Standalone chitosan nanoparticles @ 2.0 g L^{-1} (T8) produced only 1.9 kg/plot across both seasons, reaffirming that chitosan alone has limited capacity to improve yields [32]. The untreated control (T9) had the lowest yields, at 1.6 kg/plot in season 1 and 1.5 kg/plot in season 2, highlighting the critical role of effective disease management strategies for achieving optimal rice production.

Chitosan nanoparticles (ChNPs) have emerged as a promising, biodegradable, and ecofriendly solution for agricultural applications. Derived from partially or fully deacetylated chitin, ChNPs exhibit unique properties, including their roles as growth promoters, antifungal agents, and nutrient carriers. Previous studies demonstrated that ChNPs significantly enhance rice yields through seed, soil, and foliar applications, with combination treatments yielding the most notable improvements [16, 31]. The cellular uptake and mechanisms of ChNPs improve nutrient absorption and activate plant defense systems [56]. Additionally, biosynthesized ChNPs have shown potent antimicrobial activity. For instance, Sathiyabama *et al.* [78] demonstrated their effectiveness against key rice pathogens, such as *P. grisea* and *Xanthomonas oryzae*. In detached leaf assays, ChNPs significantly reduced the incidence of rice blast and bacterial blight, underscoring their potential in integrated pest management systems. By enhancing nutrient uptake, stimulating growth-promoting pathways, and activating defense responses against pathogens, ChNPs contribute to improved plant health and resilience. Furthermore, their controlled release mechanisms ensure consistent nutrient availability, enabling sustained productivity gains while minimizing environmental impacts.

Interaction analysis of the yield obtained in the both seasons, revealed the consistent efficacy of HECNPs across varying environmental conditions, with T6 (HECNPs @ 12.5 g a.i. ha^{-1}, two sprays) outperforming other treatments in both cropping seasons. This consistency underscores the robustness of HECNPs in delivering sustained productivity benefits under diverse seasonal and disease pressures. The superior performance of HECNPs can be attributed to their enhanced bioavailability, controlled release properties, and improved plant penetration [14, 45].

This study underscores the promise of HECNPs as an innovative and sustainable alternative to commercial fungicides for rice blast management and yield enhancement. Future research on the long-term effects of HECNPs on soil health, microbial diversity, and crop resilience is warranted. While ChNPs have shown immense potential, challenges related to scalability, economic feasibility, and formulation optimization must be addressed. Research efforts should focus on enhancing delivery systems and reducing production costs to enable widespread adoption of ChNP-based technologies.

Future research should explore the integration of advanced multi-omics techniques and conduct long-term field studies to refine nanoparticle formulations and assess their scalability in sustainable agricultural practices. In conclusion, while nanoparticles demonstrate significant potential as agricultural tools, their efficacy are concentration-dependent, requiring precise management to balance their growth-promoting and stress-mitigating effects with environmental safety. Further exploration and optimization will enable their broader application in addressing global agricultural challenges.

Conclusion

Notably, HECNPs demonstrated superior antifungal activity at significantly lower concentrations than commercial hexaconazole, with a reduced lethal dose (EC_{50}) value, indicating enhanced potency. Field trials conducted over two consecutive cropping seasons (rabi, 2022-23 and rabi, 2023-24) validated the superior efficacy of HECNPs in controlling rice blast disease. The most effective disease suppression and yield improvement were achieved with two HECNP applications at 12.5 g a.i. ha^{-1}, significantly outperforming conventional hexaconazole treatments. These results confirm the potential of HECNPs in reducing disease severity and thereby improving rice productivity. Economic assessments demonstrated that HECNP applications resulted in higher net returns compared to commercial hexaconazole. The reduced application rates required for HECNPs, coupled with their enhanced efficacy, establish them as a cost-effective alternative for farmers, aligning with sustainable agricultural practices.

Declarations

Ethical Approval

This research did not involve human participants or animals. Clinical Trail number : Not applicable

Consent to Participate

All authors consented to participate in this study.

Consent to Publish

All authors read and approved the final manuscript for publication.

Author Contributions

Kiran Kumar N. and Anil Kumar P. formulated the working hypothesis, conducted the experiments, collected the data, and drafted the manuscript. Prasad T. N. V. K. V. supervised the laboratory work, including the synthesis of nanoparticles. Madhusudhan P. supervised the field evaluation of nanoparticles. Jasudasu G. S. and Devaki K. monitored the characterization of nanoparticles. Sreenivasa Rao Ch. and Sreekanth B. analyzed the data and critically revised the manuscript.

Funding

The authors received no specific financial support for this work.

Competing Interests

The authors declare that they have no known competing financial interests or personal relationships that could have influenced the work reported in this paper.

Availability of data and materials

The data of the current research will be made available upon on reasonable request.

Clinical trial number

Not applicable

References

1. Abdel-Megeed RM. Biogenic nanoparticles as a promising drug delivery system. Toxicol Rep. 2024;14:101887. 10.1016/j.toxrep.2024.101887.
2. Abidin ZNA, Kormin F, Zainol Abidin NA, Bakar MFA, Moujdin IA. Synthesis and characterization of curcumin-chitosan loaded gold nanoparticles by *Oryctes rhinoceros*' chitin for cosmeceutical application. Molecules. 2023;284:1799. 10.3390/molecules28041799.
3. Alghuthaymi M, Hassan A, Kalia A, Ahl R, Elhamaky A, Oleksak P, Kuca K, Abd-Elsalam K. Antifungal nano-therapy in veterinary medicine: Current status and future prospects. J Fungi. 2021;77:494. 10.3390/jof7070494.
4. Alghuthaymi MA, Almoammar H, Rai M, Said-Galiev E, Abd-Elsalam KA. Myconanoparticles: Synthesis and their role in phytopathogens management. Biotechnol Biotechnol Equip. 2015;29(2):221–36. 10.1080/13102818.2015.1008194.
5. Amoghavarsha C, Devanna P, Chidanandappa E, Huded S, Adke R, Kumar MK, Rajashekara H, Alase S. Chemicals for the management of paddy blast disease. In *Recent Advances in Rice Research for Food, Nutrition and Security*. Chapter. 2021;5. 10.1007/978-3-030-60585-8_5.
6. Anastassiades M, Scherbaum E, Taşdelen B, Stajnbaher D. 2007. Recent developments in QuEChERS methodology for pesticide multiresidue analysis. In H. Ohkawa, H. Miyagawa and P. W. Lee Eds. *Pesticide Chemistry*. 10.1002/9783527611249.ch46
7. Anderson AL, Henry BW, Tullis EC. Factors affecting infectivity, spread and persistence of *Piricularia oryzae* Cav. Phytopathology. 1947;37(2):94–110.
8. Aziz A, Shaikh H, Abbas A, Zehra KE, Javed B. Microscopic techniques for nanomaterials characterization: A concise review. Microsc Res Tech. 2025. 10.1002/jemt.24799.
9. Barrera-Mendez F, Sanchez D, Rangel D, Haas J, Villanueva J, Olivares Romero JL. Propiconazole nanoencapsulation in biodegradable polymers to obtain pesticide-controlled delivery systems. J Mex Chem Soc. 2019;63(1):53–60. 10.29356/jmcs.v63i1.564.
10. Basumallick S. Synthesis of biocompatible chitosan nanoparticles by some greener methods for drug encapsulations. Hand book of Consumer Nanoproducts. Springer; 2022. pp. 595–610. 10.1007/978-981-16-8698-6_49.
11. Bonman JM. Durable resistance to rice blast disease-environmental influences. Euphytica. 1992;63:115–23. 10.1007/BF00023917.
12. Chai LK, Mohd-Tahir N, Bruun-Hansen HC. Dissipation of acephate, chlorpyrifos, cypermethrin, and their metabolites in a humid-tropical vegetable production system. Pest Manag Sci. 2009;652:189–96.
13. Chen D, Liu X, Lu X, Tian J. Nanoparticle drug delivery systems for synergistic delivery of tumor therapy. Front Pharmacol. 2023;14:1111991. 10.3389/fphar.2023.1111991.
14. Chen J, Wu L, Lu M, Lu S, Li Z, Ding W. Comparative study on the fungicidal activity of metallic MgO nanoparticles and macroscale MgO against soilborne fungal phytopathogens. Front Microbiol. 2020;11:365. 10.3389/fmicb.2020.00365.
15. Deepika, Prasad M, Salar A, Kumar Salar R. *vitro* anticancer activity of curcumin loaded chitosan nanoparticles CLCNPs against Vero cells. Pharmacol Res - Mod Chin Med. 2022;3:100116. 10.1016/j.prmcm.2022.100116.
16. Divya K, Thampi M, Vijayan S, Shabanamol S, Jisha MS. Chitosan nanoparticles as a rice growth promoter: Evaluation of biological activity. Arch Microbiol. 2022;204(1):95. 10.1007/s00203-021-02669-w.

17. Duse L, Pinnapireddy SR, Strehlow B, Jedelská J, Bakowsky U. Low level LED photodynamic therapy using curcumin loaded tetraether liposomes. Eur J Pharm Biopharm. 2018;12(6):233–41. 10.1016/j.ejpb.2017.10.005.
18. Dutta P, Kumari A, Mahanta M, Upamanya GK, Heisnam P, Borua S, Kaman PK, Mishra AK, Mallik M, Muthukrishnan G, Sabarinathan KG, Puzari KR, Vijayreddy D. Nanotechnological approaches for management of soil-borne plant pathogens. Front Plant Sci. 2023;14:1136233. 10.3389/fpls.2023.1136233.
19. Dwivedi K, Mandal AK, Afzal O, Altamimi ASA, Sahoo A, Alossaimi MA, Almalki WH, Alzahrani A, Barkat MA, Almeleebia TM, Mir N, Ullah SN, Rahman M. Emergence of nano-based formulations for effective delivery of flavonoids against topical infectious disorders. Gels. 2023;9(8):671. 10.3390/gels9080671.
20. Elumalai S, Santhose B, Devika R, Revathy S. Collection, isolation, identification, and biosynthesis of silver nanoparticles using microalga *Chlorella pyrenoidosa*. Nanomechanics Sci Technology: Int J. 2013;4(1):59–66. Doi: 10.1615/NanomechanicsSci Techno lIntJ.v4.i1.40.
21. Fan W, Yan W, Xu Z, Ni H. Formation mechanism of monodisperse, low molecular weight chitosan nanoparticles by ionic gelation technique. Colloids Surf B. 2012;90:21–7.
22. Fei L, Hao L. 2024. *In vitro* and *ex vivo* antifungal activities of metconazole against the rice blast fungus *Pyricularia oryzae*. *Molecules*. *29*(6): 1353. 10.3390/molecules29061353
23. Froyd J, Paget C, Guse L, Dreikorn B, Pafford J. Tricyclazole: A new systemic fungicide for control of *Pyricularia oryzae* on rice. Phytopathology. 1976;66:1135–9. 10.1094/Phyto-66-1135.
24. Gama J, Neves BC, Pereira A. Developmental inequity and the impact of pesticide exposure on gut and brain health in developing nations – a Brazilian perspective. Humanit Social Sci Commun. 2025;12:122. 10.1057/s41599-024-04229-1.
25. Gao Y, Li D, Li D, Xu P, Mao K, Zhang Y, Qin X, Tang T, Wan H, Li J, Guo M, He S. Efficacy of an adhesive nanopesticide on insect pests of rice in field trials. J Asia Pac Entomol. 2020;23(4):1222–7. 10.1016/j.aspen.2020.08.013.
26. Gawande MB, Goswami A, Felpin FX, Asefa T, Huang X, Silva R, Zou X, Zboril R, Varma RS. 2016. Cu and Cu-Based Nanoparticles: Synthesis and Applications in Catalysis. Chem Rev *116*(6): 3722–811. 10.1021/acs.chemrev.5b00482
27. Ghimire P, Bahadur KCG, Shrestha SM, Parajuli G. Evaluation of fungicides and bio-agent against neck blast disease of rice. J Plant Pathol Microbiol. 2017;8(12):1000428. 10.4172/2157-7471.1000428.
28. Gomez KA, Gomez AA. 1984. *Statistical Procedures for Agricultural Research*. 2nd Edition, John Wiley and Sons, New York, 680 p.
29. Gomez-Ramos MDM, Nannou C, Bueno M, Goday A, Murcia-Morales M, Ferrer C, Fernandez-Alba A. Pesticide residues evaluation of organic crops: A critical appraisal. Food Chemistry: X. 2020;5:100079. 10.1016/j.fochx.2020.100079.
30. Gupta R, Anand G, Pizarro L, Laor D, Kovetz N, Sela N, Yehuda T, Gazit E, Bar M. Cytokinin inhibits fungal development and virulence by targeting the cytoskeleton and cellular trafficking. mBio. 2021;12(5):e0306820. 10.1128/mBio.03068-20.
31. Hafeez R, Guo J, Ahmed T, Jiang H, Raza M, Shahid M, Ibrahim E, Wang Y, Wang J, Yan C, An Q, White J, Li B. Bio-formulated chitosan nanoparticles enhance disease resistance against rice blast by physiomorphic, transcriptional, and microbiome modulation of rice *Oryza sativa* L. Carbohydr Polym. 2024;334(3):122023. 10.1016/j.carbpol.2024.122023.
32. Hernandez-Lauzardo A, Valle M, Veranza-Castelan L, Melo-Giorgana G, Guerra-Sanchez G. Effect of chitosan on three isolates of *Rhizopus stolonifer* obtained from peach, papaya, and tomato. Fruits. 2010;65(4):245–53. 10.1051/fruits/2010020.
33. Hesami G, Darvishi S, Zarei M, Hadidi M. Fabrication of chitosan nanoparticles incorporated with *Pistacia atlantica* subsp. *kurdica* hulls' essential oil as a potential antifungal preservative against strawberry grey mould. Int J Food Sci Technol. 2021;56(9):4215–23. 10.1111/ijfs.15110.
34. Hunter RJ. Applications of the zeta potential. Zeta Potential in Colloid Science: Principles and Applications. Academic; 1988. pp. 187–257.
35. IRRI. 1996. *Standard Evaluation system for Rice*, 4th Edition, INGER Genetic Resources Center, International Rice Research Institute, Philippines, pp52.

36. Jafernik K, Ładniak A, Blicharska E, Czarnek K, Ekiert H, Wiącek AE, Szopa A. 2023. Chitosan-based nanoparticles as effective drug delivery systems-A review. *Molecules. 28*(4): 1963. 10.3390/molecules28041963
37. Jiang L, Ding L, Liu G. Nanoparticle formulations for therapeutic delivery, pathogen imaging and theranostic applications in bacterial infections. Theranostics. 2023;13(5):1545–70. 10.7150/thno.82790.
38. Kaur M, Cohen Y, Poverenov E, Eltzov E. Binding selectivity of N-alkylaminated modified chitosan nanoparticles produce a synergistic antibacterial effect against gram-negative strains. Reactive Funct Polym. 2023;18(6):105567. 10.1016/j.reactfunctpolym.2023.105567.
39. Kenneth R, Sims H Jr., Hyun K, Benoit SWD. Electrostatic Interactions Enable Nanoparticle Delivery of the Flavonoid Myricetin. ACS Omega. 2020;5(22):12649–59. 10.1021/acsomega.9b04101.
40. Kongcharoen N, Kaewsalong N, Dethoup T. Efficacy of fungicides in controlling rice blast and dirty panicle diseases in Thailand. Sci Rep. 2020;10:16233. 10.1038/s41598-020-73222-w.
41. Krishna SBN, Narasimha G. Nanofungicides: A new frontier in agriculture. Nanofungicides: Novel Applications in Plant Disease Control. Elsevier; 2023. pp. 123–37. 10.1016/B978-0-323-95305-4.00007-8.
42. Kirankumar N, Anilkumar P, Madhusudhan P, Sreekanth B, Sreenivasarao C. Evaluating alternative fungicides for effective management of rice blast disease: inhibitory effects on *Pyricularia oryzae* Cavara. J Adv Biology Biotechnol. 2024;27(10):1405–11.
43. Liu J, Yu H, Kong J, Ge X, Sun Y, Mao M, Wang DY, Wang Y. Preparation, characterization, stability, and controlled release of chitosan-coated zein/shellac nanoparticles for the delivery of quercetin. Food Chem. 2024;44(4):138634. 10.1016/j.foodchem.2024.138634.
44. Liu M, Wei X, Zheng Z, Li Y, Li M, Lin J, Yang L. Recent advances in nano-drug delivery systems for the treatment of diabetic wound healing. Int J Nanomed. 2023;27(18):1537–60. 10.2147/IJN.S395438.
45. Liu Y, Xu L, Zhang Q, Kang Y, Liu L, Liu Z, Wang Y, Jiang X, Shan Y, Luo R, Cui X, Yang Y, Yang X, Liu X, Li Z. 2022. Localized myocardial anti-inflammatory effects of temperature-sensitive budesonide nanoparticles during radiofrequency catheter ablation. AAAS *Research.* 2022: 9816234. 10.34133/2022/9816234
46. Machado TO, Beckers SJ, Fischer J, Muller B, Sayer C, de Araujo PHH, Land fester, K and, Wurm FR. 2020. Bio-based lignin nanocarriers loaded with fungicides as a versatile platform for drug delivery in plants. *Biomacromolecules. 21*(7): 2755–2763. 10.1021/acs.biomac.0c00487
47. Mahmud AMN, Rahman M, Na TW, Park JH, Yang A, Park KH, Nahar N, Shim JH. A QuEChERS-based extraction method for the residual analysis of pyraclofos and tebufenpyrad in perilla leaves using gas chromatography: Application to dissipation pattern. Biomedicinal Chromatogr. 2013;272:156–63. 10.1002/bmc.2763.
48. Marin-Silva DA, Romano N, Damonte L, Giannuzzi L, Pinotti A. Hybrid materials based on chitosan functionalized with green synthesized copper nanoparticles: Physico-chemical and antimicrobial analysis. Int J Biol Macromol. 2023;24(22):124898. 10.1016/j.ijbiomac.2023.124898.
49. Matei P, Iacomi B, Martín-Gil J, Lebena E, Ramos-Sanchez MDC, Barrio-Arredondo M, Martin-Ramos P. *vitro* antifungal activity of composites of AgNPs and polyphenol inclusion compounds against *Fusarium culmorum* in different dispersion media. Agronomy. 2018;8(11):239. 10.3390/agronomy8110239.
50. Meena HM, Kukreti S, Jassal P. Preparation, characterization of magnetic chitosan nanoparticles coated with Fe_3O_4 prepared by *ex-situ* co-precipitation method. Preprints. 2023. 10.20944/preprints202308.2130.v1.
51. Mehra M, Sheorain J, Bakshi J, Thakur R, Grewal S, Dhingra D, Kumari S. Synthesis and evaluation of berberine loaded chitosan nanocarrier for enhanced in-vitro antioxidant and anti-inflammatory potential. Carbohydr Polym Technol Appl. 2024;7:100474.
52. Ministry of Agriculture and Farmers, Welfare I. 2020. Draft Notification S.O.531E dated 03.02.2020. pp 47.
53. Mohiddin F, Bhat N, Wani S, Bhat A, Ahanger M, Shikari A, Sofi N, Parveen S, Khan G, Bashir D, Vachová P, Hassan S, El-Sabagh A. Combination of strobilurin and triazole chemicals for the management of blast disease in Mushk Budji – aromatic rice. J Fungi. 2021;7(12):1060. 10.3390/jof7121060.

54. Morones JR, Elechiguerra JL, Camacho A, Holt K, Kouri JB, Ramirez JT, Yacaman MJ. The bactericidal effect of silver nanoparticles. Nanotechnology. 2005;16(10):2346–53. 10.1088/0957-4484/16/10/059.
55. Nair RS, Morris A, Billa N, Leong CO. An evaluation of curcumin-encapsulated chitosan nanoparticles for transdermal delivery. AAPS Pharm Sci Tech. 2019;20(2):69.
56. Nandini T, Sudhalakshmi C, Sivakumar K, Parameswari E, Thangamani C. A review: Chitosan nanoparticles towards enhancing nutrient use efficiency in crops. Int J Biol Macromol. 2025;306(2):141433. 10.1016/j.ijbiomac.2025.141433.
57. Netam RS, Bahadur AN, Tiwari U, Tiwari RKS. Efficacy of plant extracts for the control of *Pyricularia grisea* blast of rice under field condition of Bastar, Chhattisgarh. Res J Agricultural Sci. 2011;2(2):269–71.
58. Nguyen M, Olson R, Shukla M, VanOeffelen M, Davis JJ. Predicting antimicrobial resistance using conserved genes. PLoS Comput Biol. 2020;16(10):e1008319. 10.1371/journal.pcbi.1008319.
59. Nino-Martinez N, Orozco MFS, Martinez-Castanon GA, Mendez FT, Ruiz F. Molecular mechanisms of bacterial resistance to metal and metal oxide nanoparticles. Int J Mol Sci. 2019;20(11):2808. 10.3390/ijms20112808.
60. Nirmal A, Shambhu K. Evaluation of triazole and strobilurin fungicides against leaf and panicle blast of rice in farmer's field. J Plant Prot Soc. 2023;86–94. 10.3126/jpps.v8i1.56450.
61. Nizamani MM, Hughes AC, Zhang HL, Wang Y. Revolutionizing agriculture with nanotechnology: Innovative approaches in fungal disease management and plant health monitoring. Sci Total Environ. 2024;928:172473. 10.1016/j.scitotenv.2024.172473.
62. Orina A, Gavrilova O, Gagkaeva T. 2020. The effect of fungicides on growth of *Fusarium* fungi in vitro. *BIO Web of Conferences. 18*: 00022. 10.1051/bioconf/20201800022
63. Ohya Y, Shiratani M, Kobayashi H, Ouchi T. Release behavior of 5-fluorouracil from chitosan-gel nanospheres immobilizing 5-fluorouracil coated with polysaccharides and their cell specific cytotoxicity. J Macromolecular Sci Part A: Pure Appl Chem. 1994;31(5):629–42. 10.1080/10601329409349743.
64. Ou SH. 1985. *Rice diseases* 2nd edition. Commonwealth Mycological Institute. P-380.
65. Paramasivam M. Determination of synthetic pyrethroids and hexaconazole residues in curry leaves and decontamination through household techniques. J Food Sci Technol. 2022;59(4):1549–57. 10.1007/s13197-021-05165-7.
66. Paramasivam M, Atchaya K, Meenakshi B, Kalaiselvi N. Residue behavior, dietary and ecological risk assessment of oxadiazine insecticide indoxacarb in chili and soil under field condition using GC-MS. Soil Sediment Contamination: Int J. 2023;32(5):557–69.
67. Parmar KD, Kalasariya RL, Litoriya NS, Chawla S, Vaghela KM, Shah PG. Development, validation, and evaluation of matrix effect of a QuEChERS-based multiresidue method with low-temperature dispersive clean-up for analysis of 104 pesticides in cumin *Cuminum cyminum* by LC-MS/MS. J Sci Food Agric. 2022;102:1782–811. 10.1002/jsfa.11515.
68. Patel S, Bajpai J, Saini R, Bajpai AK, Acharya S. Sustained release of pesticide Cypermethrin from nanocarriers: An effective technique for environmental and crop protection. Process Saf Environ Prot. 2018;117:315–25. 10.1016/j.psep.2018.05.012.
69. Perestrelo R, Silva P, Porto-Figueira P, Pereira JAM, Silva C, Medina S, Camara JS. QuEChERS - Fundamentals, relevant improvements, applications, and future trends. Anal Chim Acta. 2019;1070:1–28. 10.1016/j.aca.2019.02.036.
70. Poshina DN, Rakshina AD, Skorik YA. Hydrophobic chitosan derivatives for gene and drug delivery in cancer therapies. Polysaccharides. 2025;6(1):11. 10.3390/polysaccharides6010011.
71. Pramesh D, Baganal M, Muniraju KM, Kenganal M, Guruprasad GS, Mahantashivayogayya K, Chethana B. Bio-efficacy of a combination fungicide against blast and sheath blight diseases of paddy. J Experimental Agric Int. 2017;14(1):1–8. 10.9734/JEAI/2016/28893.
72. Purohit SD, Priyadarshi R, Bhaskar R, Han SS. Chitosan-based multifunctional films reinforced with cerium oxide nanoparticles for food packaging applications. Food Hydrocolloids. 2023;14(3):108910. 10.1016/j.foodhyd.2023.108910.

73. Qiu J, Chen Y, Liu Z, Wen H, Jiang N, Shi H, Kou Y. The application of zinc oxide nanoparticles: An effective strategy to protect rice from rice blast and abiotic stresses. Environ Pollut. 2023;33(11):121925. 10.1016/j.envpol.2023.121925.
74. Rajashekaraiah R, Kumar PR, Prakash N, Rao GS, Devi VR, Metta M, Narayanaswamy HD, Swamy MN, Satyanarayan K, Rao S, Rathnamma D, Sahadev A, Sunilchandra U, Santhosh CR, Dhanalakshmi H, Kumar SN, Ruban SW, Kalmath GP, Gomes AR, Kumar KRA, Govindappa PK. Anticancer efficacy of 6-thioguanine loaded chitosan nanoparticles with or without curcumin. Int J Biol Macromol. 2020;14(8):704–14. 10.1016/j.ijbiomac.2020.01.117.
75. Rangaraj S, Gopalu K, Muthusamy P, Venkatachalam R, Narayanasamy K. Augmented biocontrol action of silica nanoparticles and *Pseudomonas fluorescens* bioformulant in maize *Zea mays* L. RSC Adv. 2014;41(5):8461–5. 10.1039/c3ra46251j.
76. Samuel U, Guggenbichler JP. Prevention of catheter-related infections: The potential of a new nano-silver impregnated catheter. Int J Antimicrob Agents. 2004;23(Supplement 1):75–8. 10.1016/j.ijantimicag.2003.12.004.
77. Sarlak N, Taherifar A, Salehi F. Synthesis of nanopesticides by encapsulating pesticide nanoparticles using functionalized carbon nanotubes and application of new nanocomposite for plant disease treatment. J Agric Food Chem. 2014;62(21):4833–8.
78. Sathiyabama M, Boomija RV, Muthukumar S, Gandhi S, Salma S, Prinsha TK, Rengasamy B. Green synthesis of chitosan nanoparticles using tea extract and its antimicrobial activity against economically important phytopathogens of rice. Sci Rep. 2024;14:7381. 10.1038/s41598-024-58066-y.
79. Shah MA, Shahnaz T, Zehab-ud-Din JHM, Masoodi S, Nazir S, Qurashi A, Hayderahmed G. Application of nanotechnology in the agricultural and food processing industries: A review. Sustainable Mater Technol. 2024;39:e00809. 10.1016/j.susmat.2023.e00809.
80. Sharma A, Sood K, Kaur J, Khatri M. Agrochemical-loaded biocompatible chitosan nanoparticles for insect pest management. Biocatal Agric Biotechnol. 2019;18:101079. 10.1016/j.bcab.2019.101079.
81. Sharma S, Sahu B, Cao L, Bindra P, Kaur K, Chandel M, Koratkar N, Huang Q, Shanmugam V. Porous nanomaterials: Main vein of agricultural nanotechnology. Prog Mater Sci. 2021;121:100812. 10.1016/j.pmatsci.2021.100812.
82. Sridevi H, Bhat MR, Kumar PS, Kumar NM, Selvaraj R. Structural characterization of cuboidal α-Fe2O3 nanoparticles synthesized by a facile approach. Appl Nanosciences. 2023;13(3):1–9. 10.1007/s13204-023-02780-y.
83. Tang Z, Zhang X, Shu Y, Guo M, Zhang H, Tao W. Insights from nanotechnology in COVID-19 treatment. Nano Today. 2021;36:101019. 10.1016/j.nantod.2020.101019.
84. United States Department of Agriculture USDA. World agricultural production. U.S. Department of Agriculture, Foreign Agricultural Service, Office of Global Analysis, International Production Assessment Division IPAD; 2024.
85. Verma P, Bodh S, Thakur S. Nanotechnology in agriculture: A review. Int J Chem Stud. 2020a;7(4):488–91.
86. Verma DK, Patel S, Kushwah K. Effects of nanoparticles on seed germination, growth, phytotoxicity, and crop improvement. Agricultural Reviews. 2020b;42(1):1–11. 10.18805/ag.R-1964.
87. Vincent JM. Distortion of fungal hyphae in presence of certain inhibition. Nature. 1947;159(4051):850–6. 10.1038/159850b0.
88. Wheeler BEJ. 1969. *An Introduction to Plant Diseases*. *Wiley and Sons*, London. 374.
89. Wilcoxson RD, Skovmand B, Atif AH. Evaluation of wheat cultivars for ability to retard development of stem rust. Ann Appl Biol. 1975;80(3):275–81. 10.1111/j.1744-7348.1975.tb01633.x.
90. Woloshuk CP, Sisler HD. Tricyclazole, pyroquilon, tetrachlorophthalide, PCBA, coumarin and related compounds inhibit melanization and epidermal penetration by *Pyricularia oryzae*. J Pesticide Sci. 1982;7:161–7.
91. Worrall EA, Bravo-Cazar A, Nilon AT, Fletcher SJ, Robinson KE, Carr JP, Mitter N. Exogenous application of RNAi-inducing double-stranded RNA inhibits aphid-mediated transmission of a plant virus. Front Plant Sci. 2019;10:265. 10.3389/fpls.2019.00265.

92. Yegireddy M, Nadoor P, Rao S, Hanumanthu PB, Rajashekaraiah R, Ramachandrappa SC, Halemani GM, Mannem S, Prasad TNVKV, Ubaradka S. Chitosan encapsulated meloxicam nanoparticles for sustained drug delivery applications: Preparation, characterization, and pharmacokinetics in Wistar rats. Molecules. 2022;27(21):7312. 10.3390/molecules27217312.
93. Yin J, Su X, Yan S, Shen J. Multifunctional nanoparticles and nanopesticides in agricultural application. Nanomaterials Basel. 2023;137:1255. 10.3390/nano13071255.
94. Yu C, Fan CQ, Chen YX, Guo F, Rao HH, Che PY, Zuo CJ, Chen HW. Global research trends and emerging hotspots in nano-drug delivery systems for lung cancer: A comprehensive bibliometric analysis 1998–2024. Discovery Oncol. 2025;16(1):33. 10.1007/s12672-025-01782-2.
95. Zainab R, Hasnain M, Ali F, Abideen Z, Siddiqui ZS, Jamil F, Hussain M, Park YK. Prospects and challenges of nanopesticides in advancing pest management for sustainable agricultural and environmental service. Environ Res. 2024;261:119722. 10.1016/j.envres.2024.119722.
96. Zhang S, He Z, Zeng M, Chen J. Impact of matrix species and mass spectrometry on matrix effects in multi-residue pesticide analysis based on QuEChERS-LC-MS. Foods. 2023;12(6):1226. 10.3390/foods12061226.
97. Zhang W, Chen H, Han X, Yang Z, Tang M, Zhang J, Zeng S, Hu D. Determination and analysis of the dissipation and residue of cyprodinil and fludioxonil in grape and soil using a modified QuEChERS method. Environ Monit Assess. 2015;187:4661. 10.1007/s10661-015-4661-9.
98. Zhao L, Ding X, Khan IM, Yue L, Zhang Y, Wang Z. Preparation and characterization of curcumin/chitosan conjugate as an efficient photodynamic antibacterial agent. Carbohydr Polym. 2023;313:120852. 10.1016/j.carbpol.2023.120852.

Figures

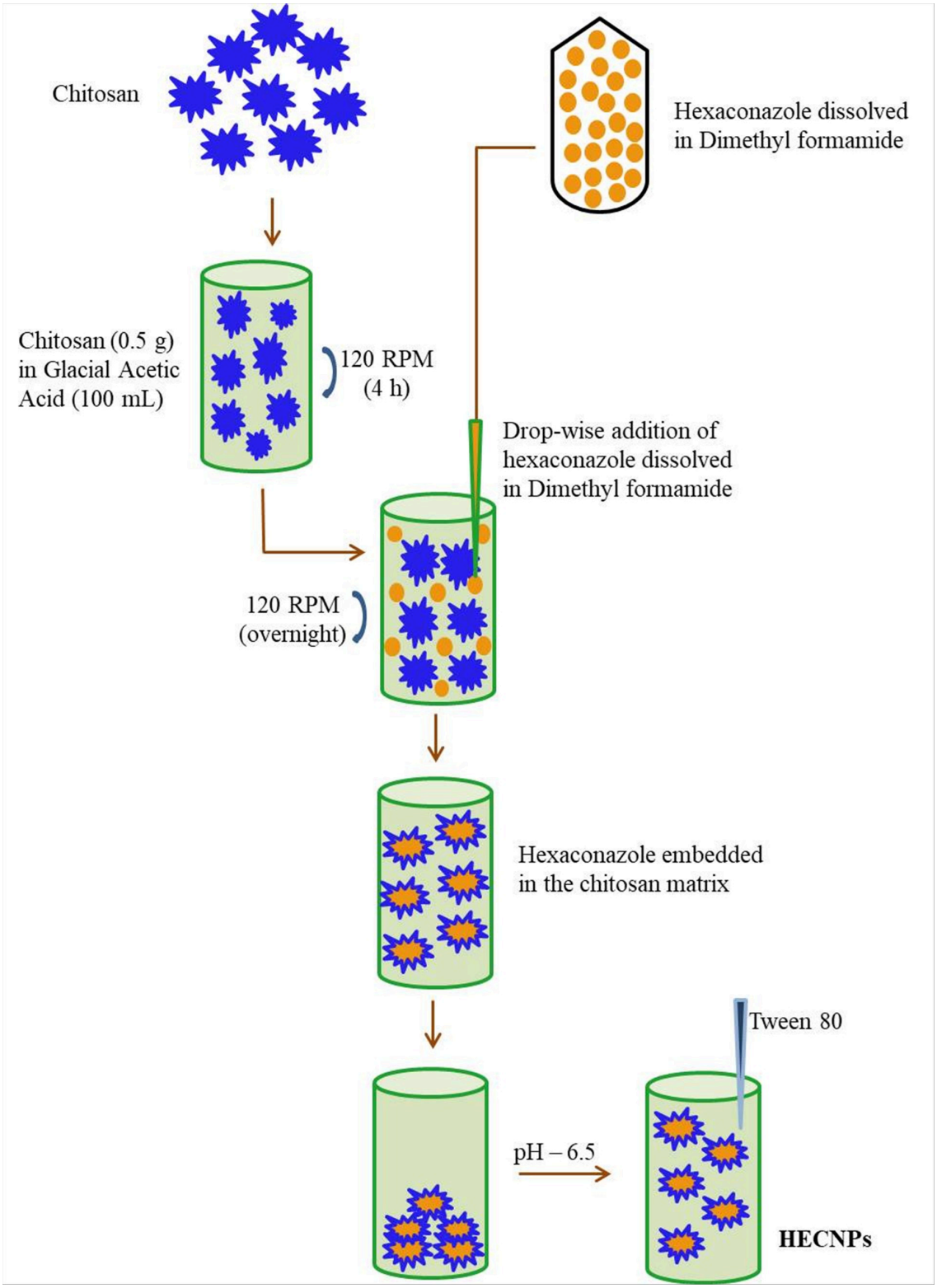


Figure 1

Preparation of HECNPs



Figure 2

Symptoms of Rice leaf blast (elongated spindle shaped lesions)

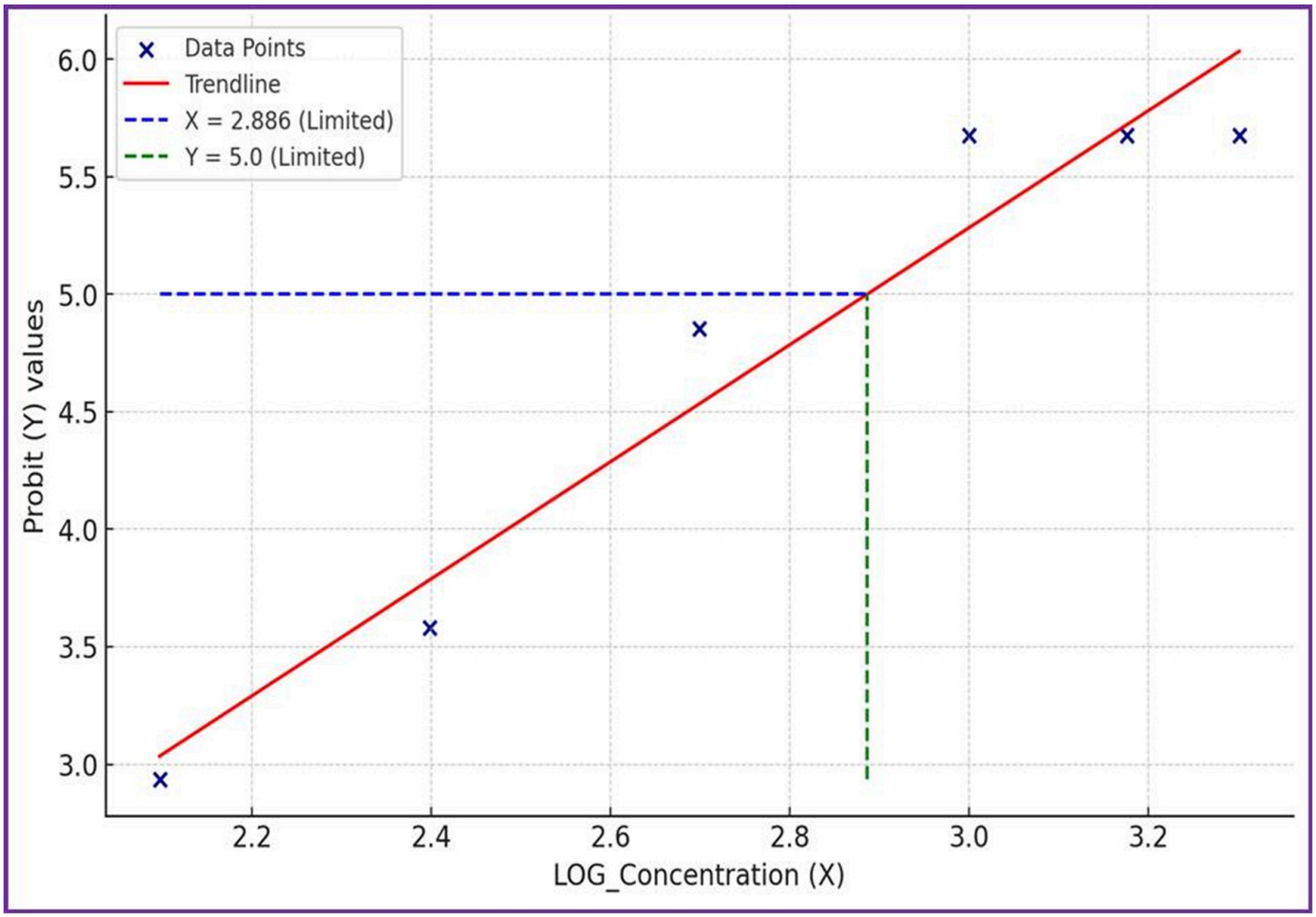


Figure 3

Calculation of EC_{50} values of Commercial Hexaconazole by Probit Analysis

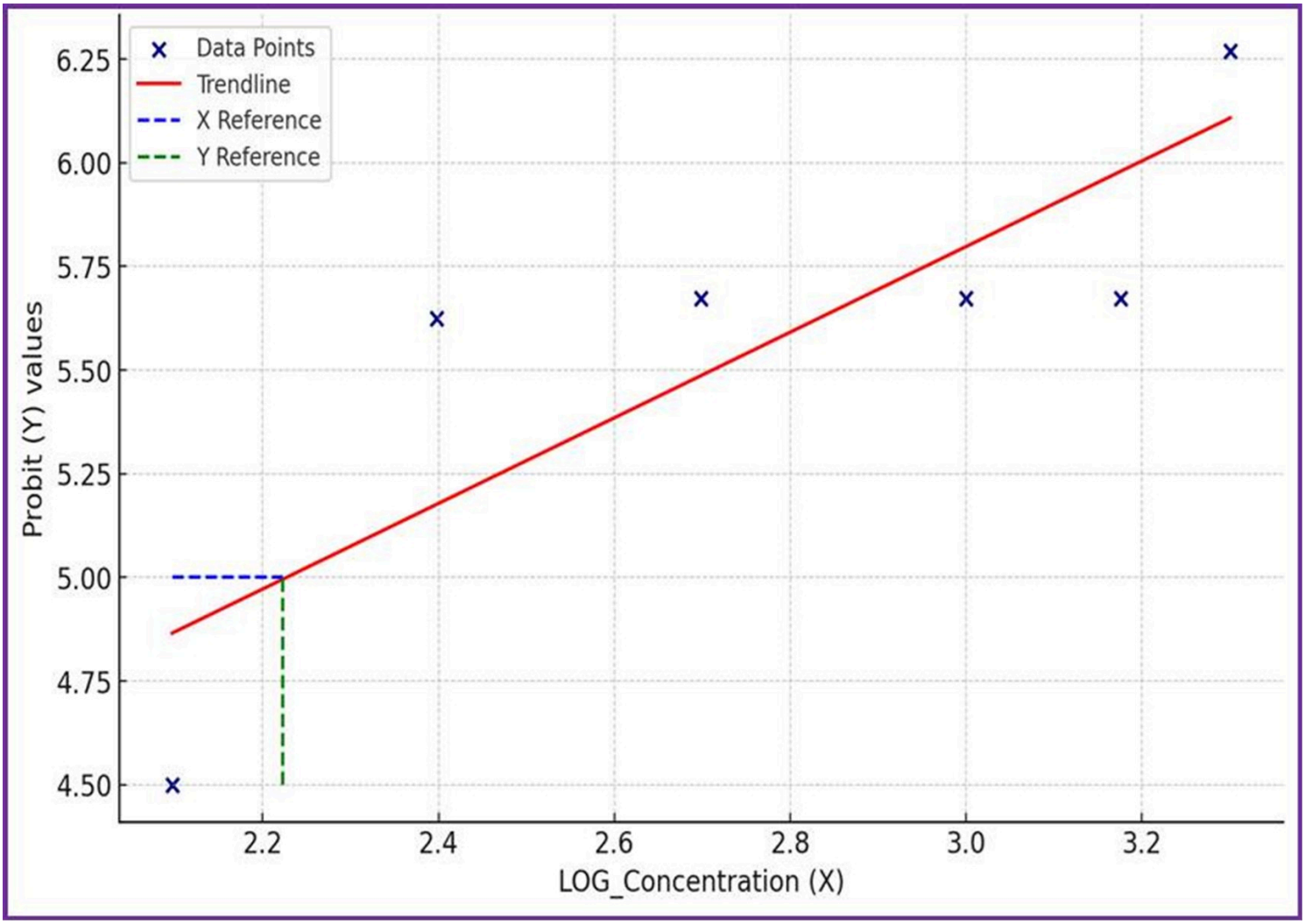


Figure 4

Calculation of EC_{50} values of HECNPs by Probit Analysis

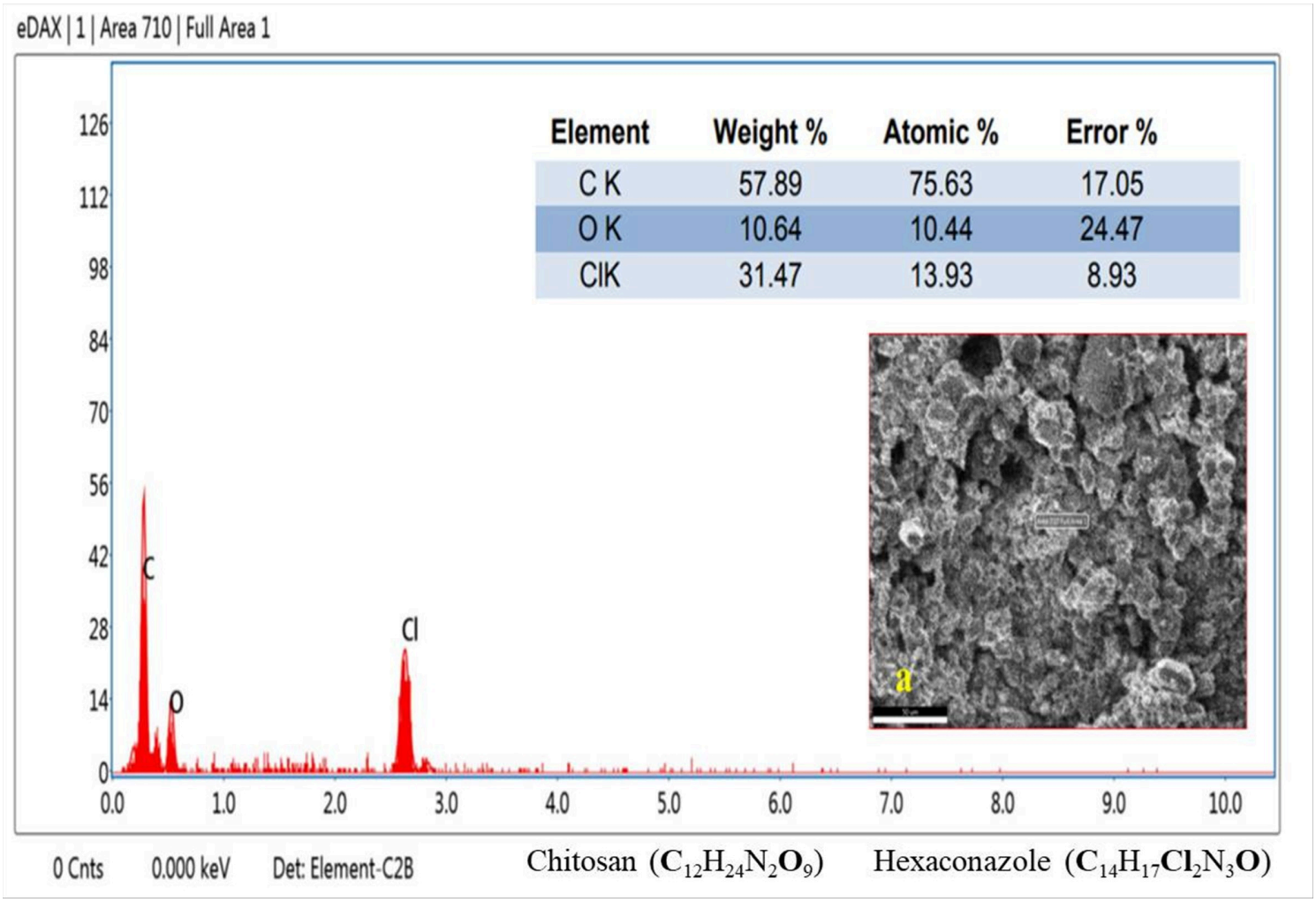


Figure 5

Energy Dispersive Spectroscopy analysis of HECNPs

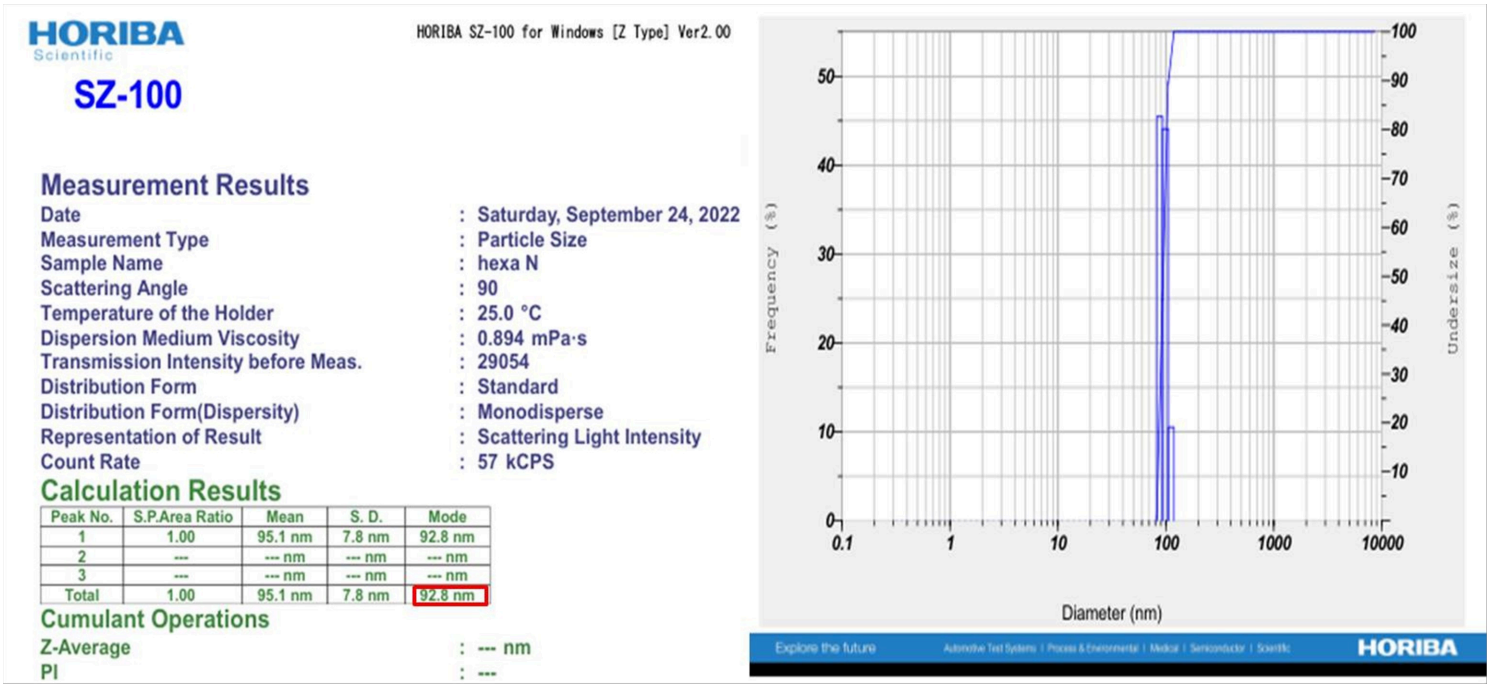


Figure 6

Hydrodynamic diameter of HECNPs

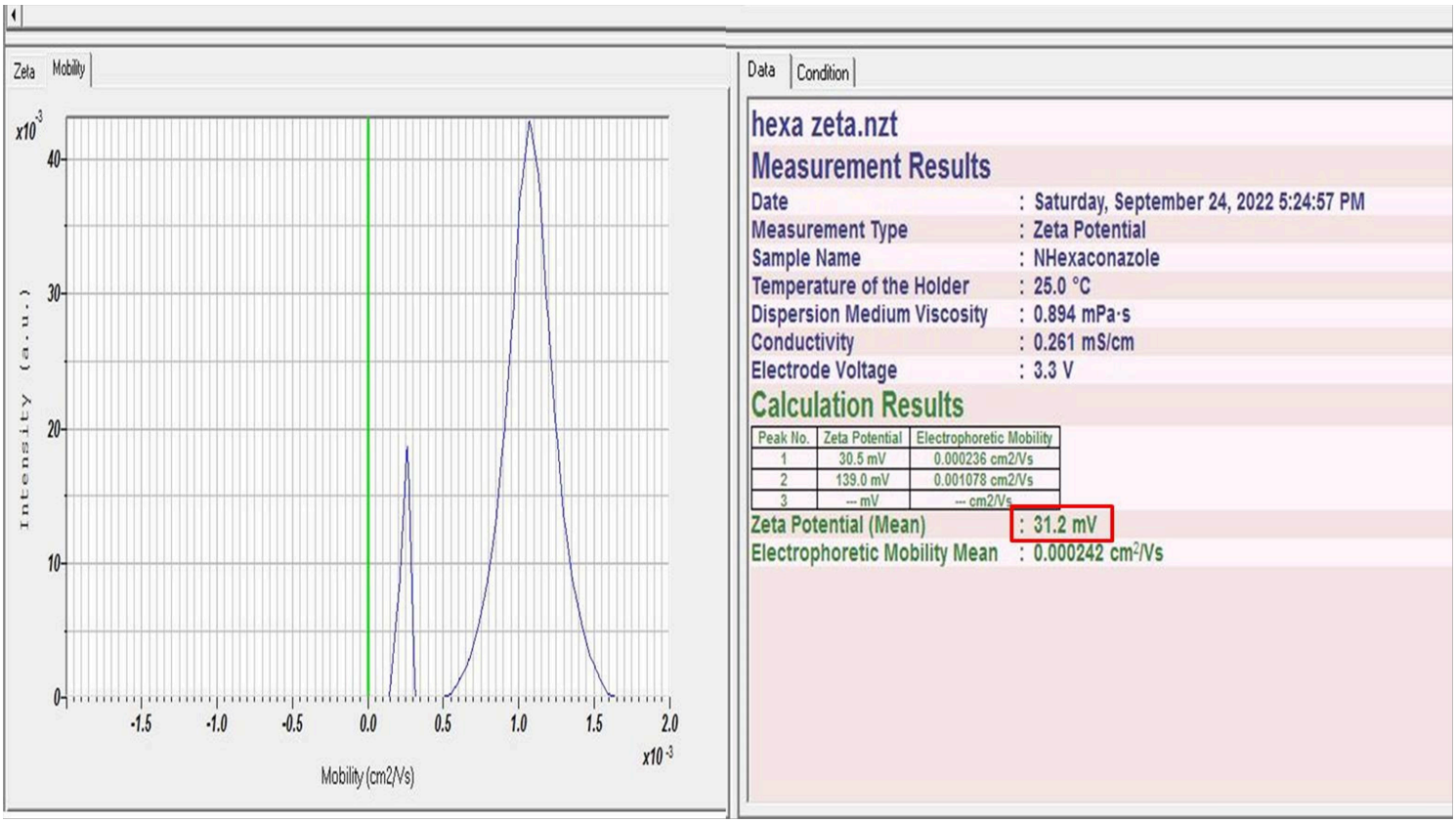


Figure 7

Zeta Potential of HECNPs

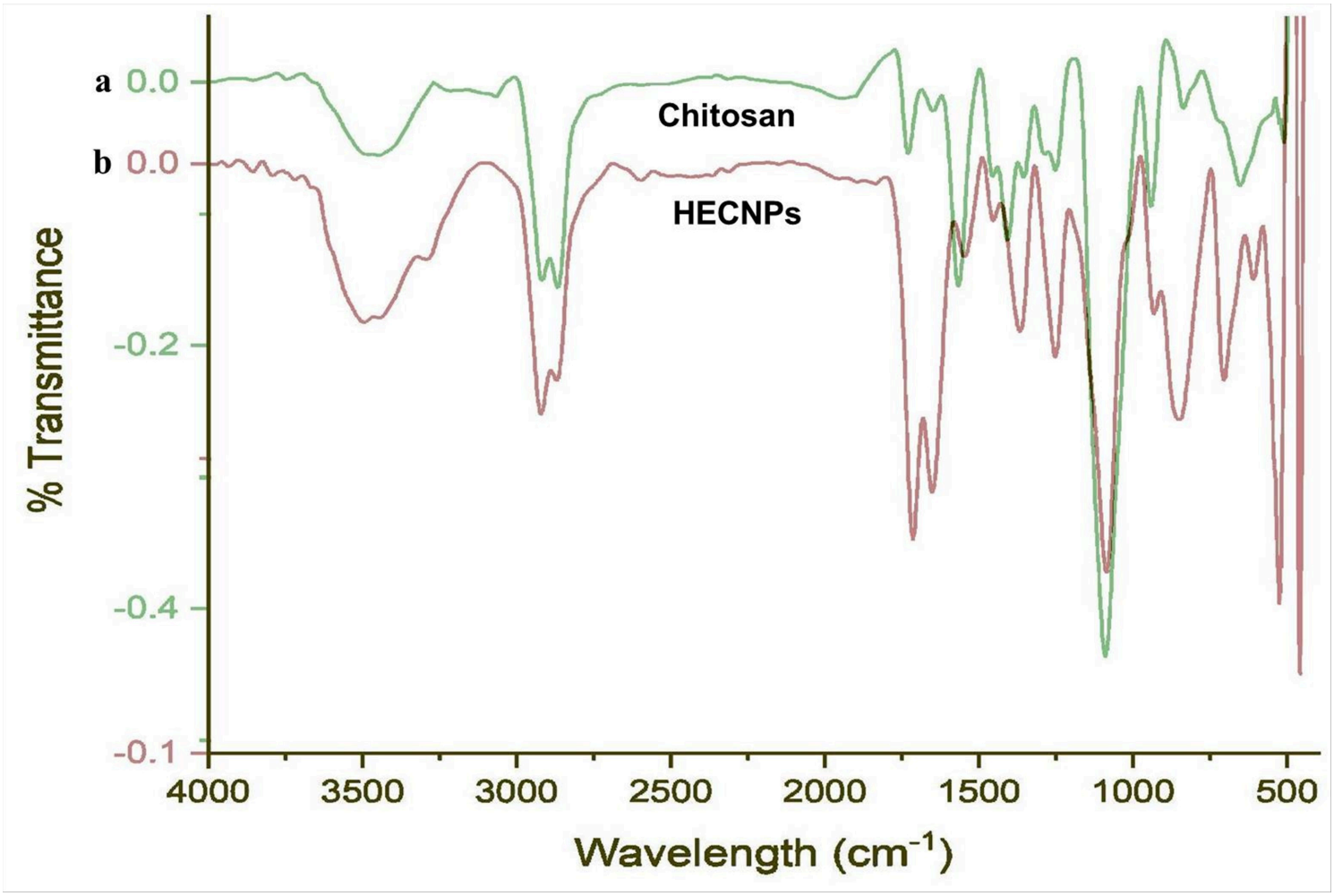


Figure 8

FT-IR spectral analysis of chitosan nano particles (green line) and HECNPs (brown line)

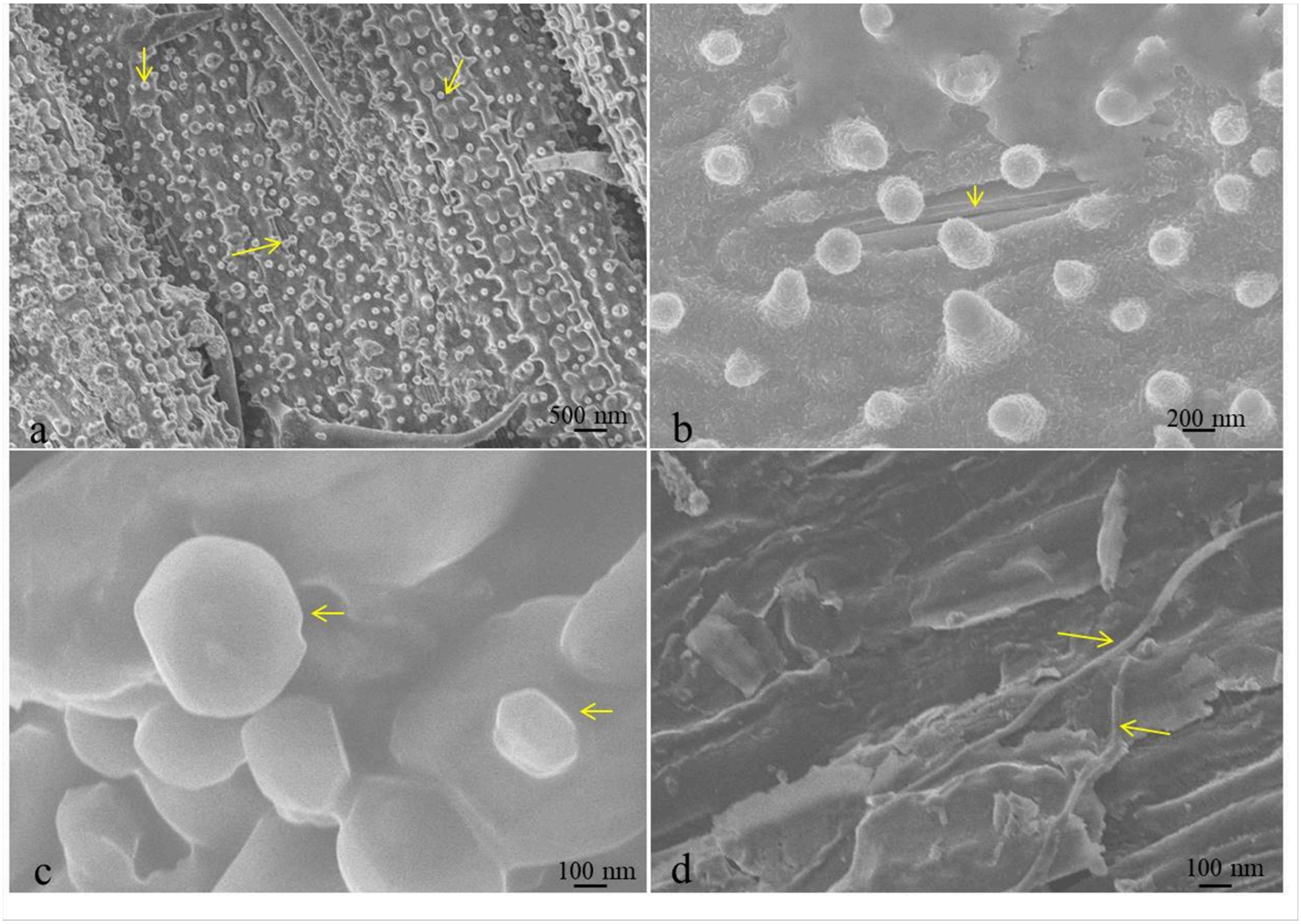
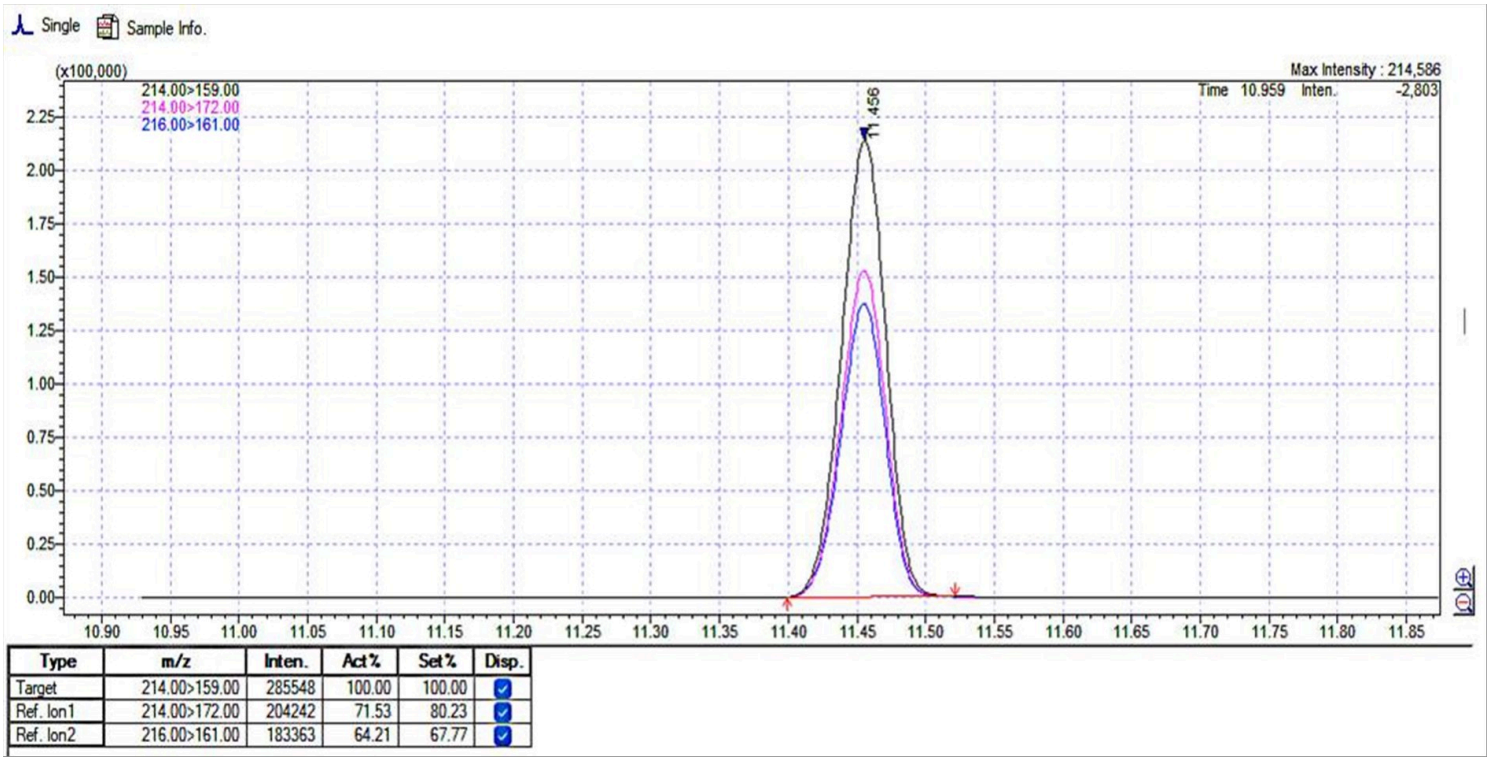


Figure 9

Scanning Electron Microscopy images of HECNPs at 500 nm (a), 200 nm (b), 100 nm (c and d)



Type	m/z	Inten.	Act%	Set%	Disp.
Target	214.00>159.00	285548	100.00	100.00	☑
Ref. Ion1	214.00>172.00	204242	71.53	80.23	☑
Ref. Ion2	216.00>161.00	183363	64.21	67.77	☑

Figure 10

Gas Chromatography-Mass Spectrometry (GC-MS) analysis of Hexaconazole

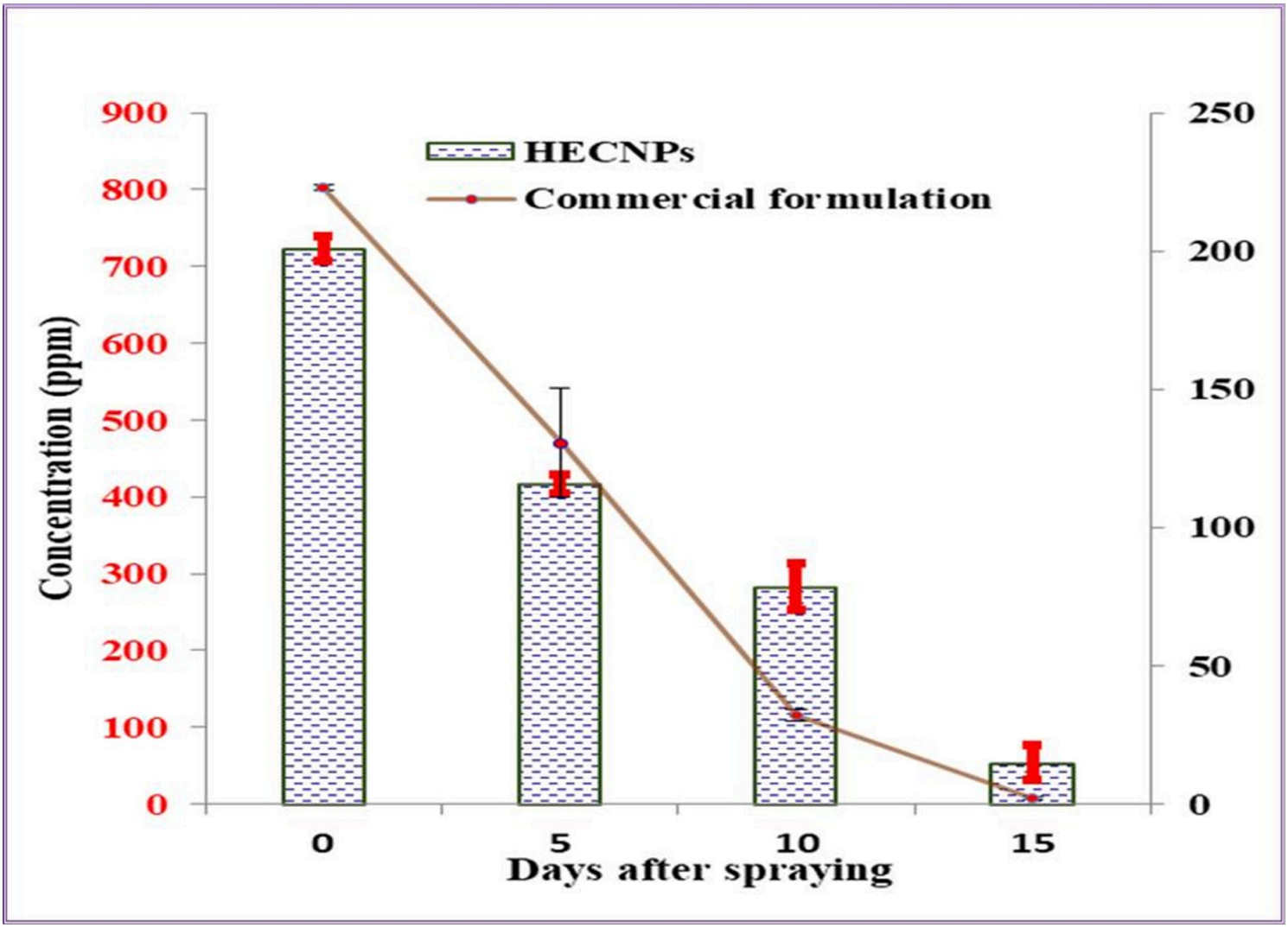


Figure 11

Determination of hexaconazole concentration in paddy leaves at different days after application of HECNPs (dotted boxes and concentrations on right side) and commercial hexaconazole (brown line and concentrations on left side)

Supplementary Files

This is a list of supplementary files associated with this preprint. Click to download.

- Supplementarytable.doc
- Supplementaryfigure.doc